ELECTRIFY THE WORLD

EPRI

BWRVIP BWR Vessel & Internals Project 2005-125

March 11, 2005

Document Control Desk
U. S. Nuclear Regulatory Commission
11555 Rockville Pike
Rockville, MD 20852

Attention: Meena Khanna

Subject: Project No. 704 – BWRVIP-114NP: BWR Vessel and Internals Project, RAMA Fluence Methodology Theory Manual

Reference: Letter from Carl Terry (BWRVIP) to Document Control Desk (NRC), "Project 704 – BWRVIP-114: BWR Vessel and Internals Project, RAMA Fluence Methodology Theory Manual," dated June 11, 2003.

Enclosed are two (2) copies of the report "BWRVIP-114NP: BWR Vessel and Internals Project, RAMA Fluence Methodology Theory Manual," EPRI Technical Report 1003660NP, March 2005. This is a non-proprietary version of the proprietary document submitted to the NRC by the letter referenced above.

If you have any questions on this subject please call Robin Dyle (Southern Nuclear, BWRVIP Integration Committee Technical Chairman) at 205.992.5882.

Sincerely,

William A Eaton

William A. Eaton
Entergy Operations, Inc.
Chairman, BWR Vessel and Internals Project

D058

Copy forwarded to Meena Khanna

CORPORATE HEADQUARTERS
3412 Hillview Avenue | Palo Alto CA 94304-1395 USA | 650.855.2000 | Customer Service 800.313.3774 | www.epri.com

EPRI

BWRVIP-114NP: BWR Vessel and Internals Project RAMA Fluence Methodology Theory Manual

Technical Report

NON-PROPRIETARY INFORMATION

NOTICE: This report contains the non-proprietary information that is included in the proprietary version of this report. The proprietary version of this report contains proprietary information that is the intellectual property of BWRVIP utility members and EPRI. Accordingly, the proprietary report is available only under license from EPRI and may not be reproduced or disclosed, wholly or in part, by any Licensee to any other person or organization.

BWRVIP-114NP: BWR Vessel and Internals Project

RAMA Fluence Methodology Theory Manual

1003660NP

Final Report, March 2005

EPRI Project Manager
R. Carter

EPRI • 3412 Hillview Avenue, Palo Alto, California 94304 • PO Box 10412, Palo Alto, California 94303 • USA
800.313.3774 • 650.855.2121 • askepri@epri.com • www.epri.com

DISCLAIMER OF WARRANTIES AND LIMITATION OF LIABILITIES

THIS DOCUMENT WAS PREPARED BY THE ORGANIZATION(S) NAMED BELOW AS AN ACCOUNT OF WORK SPONSORED OR COSPONSORED BY THE ELECTRIC POWER RESEARCH INSTITUTE, INC. (EPRI). NEITHER EPRI, ANY MEMBER OF EPRI, ANY COSPONSOR, THE ORGANIZATION(S) BELOW, NOR ANY PERSON ACTING ON BEHALF OF ANY OF THEM:

(A) MAKES ANY WARRANTY OR REPRESENTATION WHATSOEVER, EXPRESS OR IMPLIED, (I) WITH RESPECT TO THE USE OF ANY INFORMATION, APPARATUS, METHOD, PROCESS, OR SIMILAR ITEM DISCLOSED IN THIS DOCUMENT, INCLUDING MERCHANTABILITY AND FITNESS FOR A PARTICULAR PURPOSE, OR (II) THAT SUCH USE DOES NOT INFRINGE ON OR INTERFERE WITH PRIVATELY OWNED RIGHTS, INCLUDING ANY PARTY'S INTELLECTUAL PROPERTY, OR (III) THAT THIS DOCUMENT IS SUITABLE TO ANY PARTICULAR USER'S CIRCUMSTANCE; OR

(B) ASSUMES RESPONSIBILITY FOR ANY DAMAGES OR OTHER LIABILITY WHATSOEVER (INCLUDING ANY CONSEQUENTIAL DAMAGES, EVEN IF EPRI OR ANY EPRI REPRESENTATIVE HAS BEEN ADVISED OF THE POSSIBILITY OF SUCH DAMAGES) RESULTING FROM YOUR SELECTION OR USE OF THIS DOCUMENT OR ANY INFORMATION, APPARATUS, METHOD, PROCESS, OR SIMILAR ITEM DISCLOSED IN THIS DOCUMENT.

ORGANIZATION(S) THAT PREPARED THIS DOCUMENT

TransWare Enterprises Inc.

NON-PROPRIETARY INFORMATION

NOTICE: This report contains the non-proprietary information that is included in the proprietary version of this report. The proprietary version of this report contains proprietary information that is the intellectual property of BWRVIP utility members and EPRI. Accordingly, the proprietary report is available only under license from EPRI and may not be reproduced or disclosed, wholly or in part, by any Licensee to any other person or organization.

ORDERING INFORMATION

Requests for copies of this report should be directed to EPRI Orders and Conferences, 1355 Willow Way, Suite 278, Concord, CA 94520, (800) 313-3774, press 2 or internally x5379, (925) 609-9169, (925) 609-1310 (fax).

Electric Power Research Institute and EPRI are registered service marks of the Electric Power Research Institute, Inc. EPRI. ELECTRIFY THE WORLD is a service mark of the Electric Power Research Institute, Inc.

Copyright © 2003 Electric Power Research Institute, Inc. All rights reserved.

CITATIONS

This report was prepared by

TransWare Enterprises Inc.
5450 Thornwood Dr. Ste. M
San Jose, CA 95123

Principal Investigator
K. E. Watkins
D. B. Jones

This report describes research sponsored by EPRI

The report is a corporate document that should be cited in the literature in the following manner:

BWRVIP-114NP: BWR Vessel and Internals Project, RAMA Fluence Methodology Theory Manual, EPRI, Palo Alto, CA: 2003 1003660NP.

PRODUCT DESCRIPTION

This report describes the theoretical and technical basis implemented in the RAMA Fluence Methodology for application to Boiling Water Reactors (BWRs).

Results & Findings

The RAMA Fluence Methodology contains the following software components: the transport code, parts model builder (PMB) code, state-point model builder (SMB) code, fluence calculator, and the nuclear data library. The methodology includes an advanced three-dimensional nuclear particle transport theory code that performs neutron and gamma flux calculations. It couples a three-dimensional, multi-group deterministic nuclear transport theory method with a combinatorial geometry modeling capability to provide a flexible and accurate tool for determining fluxes for any light water reactor design. The code supports the method of characteristics transport theory solution technique, a three-dimensional ray-tracing method, combinatorial geometry, a fixed source iterative solution, anisotropic scattering, thermal-group upscattering treatments, and a nuclear cross-section data library based upon the ENDF/B-VI data file. The software is written in conformance to the Fortran 95 programming language standard for ease of portability between computing platforms. The methodology adheres to the requirements set forth in NRC Regulatory Guide 1.190 for pressure vessel neutron fluence determinations.

Challenges & Objectives

The objectives of this project were to (1) develop a state-of-the-art method for calculating fluence in a BWR; (2) adhere to the requirements of NRC Regulatory Guide 1.190; (3) validate the methodology against specific benchmark problems identified in the regulatory guide and perform plant-specific analyses; and (4) develop a system of software codes for application by utilities.

Applications, Values & Use

The RAMA Fluence Methodology software package is used to determine neutron fluence in BWR components in compliance with the requirements and guidelines provided in U.S. Nuclear Regulatory Commission Regulatory Guide 1.190. RAMA, Version 1.0 is designed to calculate the fluence for surveillance capsules, the reactor pressure vessel within the active fuel height, and the core shroud within the active fuel height. Future versions of RAMA will be developed to extend the methodology to other internal components that are beyond the active fuel height.

EPRI Perspective

Accurate neutron fluence determinations for BWRs are required for a number of reasons: (1) to determine neutron fluence within the reactor pressure vessel (RPV) and at surveillance capsule locations to address vessel embrittlement issues; (2) to determine neutron fluence on the core shroud in order to determine fracture toughness and crack growth rate for use in flaw evaluation calculations; and (3) to determine neutron fluence at other internal components for structural integrity assessments or to evaluate repair technologies. The RAMA Fluence Methodology is a state-of-the-art and versatile tool for calculating the fluence of the BWR pressure vessel and internals.

Approach

The BWRVIP conducted an extensive review and evaluation of existing technologies employed to determine the fluence of light water reactors. The 3-dimensional nuclear particle transport theory, combinatorial geometry methods, and additional advanced features of the RAMA methodology provide capabilities not available in other existing technologies to accurately calculate the fluence of complex BWR internal components. Thus, RAMA was selected as the methodology to address the needs of the BWRVIP. A key aspect of this work was to ensure that the RAMA methodology adheres to the requirements set forth in NRC Regulatory Guide 1.190 for pressure vessel neutron fluence determinations. To accomplish this, the methodology was verified and validated against specific benchmark problems identified in the regulatory guide and plant-specific analyses were performed. Results of benchmark analyses will be presented in another BWRVIP report.

Keywords

Fluence

Embrittlement

Boiling water reactor

Vessel and internals

Reactor pressure vessel

ABSTRACT

This document describes the technical basis implemented in the RAMA Fluence Methodology software package. The RAMA Fluence Methodology contains the following software components: the transport code, parts model builder (PMB) code, state-point model builder (SMB) code, fluence calculator and the nuclear data library.

The RAMA Fluence Methodology software package is used to determine neutron fluence in BWR Priority 1 components in compliance with the requirements and guidelines provided in U.S. Nuclear Regulatory Commission Regulatory Guide 1.190. The BWR Priority 1 components include surveillance capsules, the reactor pressure vessel within the active fuel height, and the core shroud within the active fuel height.

The RAMA Fluence Methodology includes an advanced three-dimensional nuclear particle transport theory code that performs neutron and gamma flux calculations. RAMA couples a three-dimensional, multi-group deterministic nuclear transport theory method with a combinatorial geometry modeling capability to provide a flexible and accurate tool for determining fluxes for any light water reactor design. The code supports the method of characteristics transport theory solution technique, a three-dimensional ray-tracing method, combinatorial geometry, a fixed source iterative solution, anisotropic scattering, thermal-group upscattering treatments, and a nuclear cross-section data library based upon the ENDF/B-VI data file. The software is written in conformance to the Fortran 95 programming language standard for ease of portability between computing platforms.

ACKNOWLEDGMENTS

The undersigned wish to acknowledge EPRI and the Boiling Water Reactor Vessel and Internals Project (BWRVIP) for their support of the RAMA Fluence Methodology project. Special thanks are given to Robert Carter and Ken Wolfe of EPRI for their guidance, comments, and overall support in completing this document.

The undersigned also wish to acknowledge Dr. Mark Williams of Louisiana State University for providing a thorough technical review of the theory and discussions in this report and Virginia Jones of TransWare for the many hours that she contributed to making this a quality document.

Dean B. Jones, TransWare Enterprises Inc.

Kenneth E. Watkins, TransWare Enterprises Inc.

CONTENTS

1 INTRODUCTION 1-1

1.1 Utility Need 1-1

1.2 Scope 1-1

1.3 Critical Characteristics 1-2

1.4 Documentation 1-2

1.5 Requisite Skills 1-3

1.6 Quality Assurance 1-3

1.7 Target Platforms 1-3

1.8 Document Organization 1-3

2 OVERVIEW OF PROGRAM ARCHITECTURE 2-1

3 OVERVIEW OF GEOMETRY MODELING 3-1

3.1 Combinatorial Geometry Model 3-1

3.2 General Geometries 3-2

3.2.1 ARB - Arbitrary Convex Polyhedron 3-2

3.2.2 BOX - General Box 3-3

3.2.3 ELL - Ellipsoid 3-4

3.2.4 RAW - Right Angle Wedge 3-5

3.2.5 RCC - Right Circular Cylinder 3-5

3.2.6 REC - Right Elliptical Cylinder 3-6

3.2.7 RPP - Rectangular Parallelepiped 3-7

3.2.8 SPH - Sphere 3-8

3.2.9 TRC - Truncated Right Angle Cone 3-9

4 TRANSPORT METHODS 4-1

4.1 Geometry 4-1

4.1.1 Coordinate System 4-1
4.1.2 Reactor Models 4-2
4.1.3 Material Descriptions 4-4
4.2 Flux Calculation Methods 4-4
4.2.1 Particle Transport Equation 4-4
4.2.2 Characteristics Solution Methodology with Anisotropic Scattering 4-5
4.2.3 Flux Edits Methods 4-11

5 GEOMETRY MODEL BUILDING METHOD 5-1
5.1 Generating the Reactor Core Region Geometry Model 5-1
5.1.1 Fuel Assembly Meshing and Volume Calculations 5-2
5.2 Generating the Core Reflector Region Geometry Model 5-2
5.2.1 Core Reflector Meshing and Volume Calculations 5-2
5.3 Generating the Core Shroud Region Geometry Model 5-3
5.3.1 Shroud Meshing and Volume Calculations 5-3
5.4 Generating the Downcomer and Jet Pump Region Geometry Model 5-3
5.4.1 Downcomer and Jet Pump Meshing and Volume Calculations 5-3
5.5 Generating Geometry Models Containing Pipe Elements 5-4
5.5.1 Pipe Element Meshing and Volume Calculations 5-4
5.6 Radial and Azimuthal Meshing in Cylindrical Parts 5-4
5.7 Volume and Material Identifiers 5-5

6 MATERIAL PROCESSING METHOD 6-1
6.1 Fuel Assembly Homogenization 6-1
6.2 Volume Weighted Averaging 6-1
6.2.1 Homogenization of the Relative Powers 6-2
6.2.2 Homogenization of the Channel and Bypass Regions 6-5
6.3 Fuel Assembly RPP Types 6-5

7 ACTIVATION, FLUENCE, AND UNCERTAINTY METHODS 7-1
7.1 Activation Evaluation 7-1
7.1.1 Nuclide Activation 7-1
7.1.2 Accumulated Activation 7-2
7.1.3 Activation Reaction Rates 7-5

7.1.4 Reactions Per Atom 7-5
7.1.5 Equivalent ^{235}U Fission Spectrum Flux and Cross Section 7-6
7.1.6 Response Function Nuclide Number Densities and Decay Constants 7-6
7.2 Neutron Flux and Fluence Evaluations 7-6
7.2.1 Neutron Flux Energy Cutoff 7-6
7.2.2 Accumulated Neutron Fluence 7-9
7.2.3 Effective Full Power Time 7-10
7.2.4 Cumulative Power Factor 7-10
7.2.5 Average Neutron Flux 7-10
7.2.6 Rated Power Neutron Flux 7-11
7.3 Uncertainty Analysis Methodology 7-11
7.3.1 Analytical Uncertainty 7-11
7.3.2 Comparison Uncertainty 7-15
7.3.3 Combined Uncertainty 7-16
7.3.4 Best Estimate Fluence 7-17

8 NUCLEAR DATA GENERATION METHOD 8-1
8.1 BUGLE-96 Data 8-1
8.2 Nuclide Identifiers 8-1
8.3 Legendre Order of Scattering 8-2
8.4 Cross Section Generation 8-2
8.4.1 Generation of Resonance Self-shielded Actinide Cross Sections 8-3
8.4.2 Generation of Broad Group Shielded Cross Sections 8-5
8.4.3 Creation of ANISN BCD Nuclear Data 8-6
8.4.4 Generation of the RAMA Nuclear Data Library 8-7

9 REFERENCES 9-1

LIST OF FIGURES

Figure 2-1 RAMA Fluence Methodology Software Architecture Flow Diagram 2-3
Figure 3-1 Arbitrary Convex Polyhedron Geometry 3-3
Figure 3-2 General Box Geometry 3-4
Figure 3-3 Ellipsoid Geometry 3-4
Figure 3-4 Right Angle Wedge Geometry 3-5
Figure 3-5 Right Circular Cylinder Geometry 3-6
Figure 3-6 Right Elliptical Cylinder Geometry 3-7
Figure 3-7 Rectangular Parallelepiped Geometry 3-8
Figure 3-8 Sphere Geometry 3-8
Figure 3-9 Truncated Right Angle Cone Geometry 3-9
Figure 4-1 BWR Reactor Assembly Coordinate System 4-2
Figure 4-2 Cutaway View of a BWR Pressure Vessel Showing the Axial Zones 4-3
Figure 6-1 Rectangular Parallelepiped (RPP) Types 6-6
Figure 7-1 Reactor Operating History Example 7-3
Figure 8-1 SCAMPI Cross Section Processing Flow Diagram 8-4
Figure 8-2 RAMA Nuclear Data Library Generation Flow Diagram 8-5

LIST OF TABLES

Table 7-1 Default Target Nuclide Number Densities 7-8
Table 7-2 Default Product Nuclide Decay Constants 7-9
Table 7-3 Sample Input Parameter Set 7-14

1
INTRODUCTION

1.1 Utility Need

Utilities have a need for a standard methodology, acceptable to the U.S. Nuclear Regulatory Commission (NRC), that can be used to perform accurate neutron fluence calculations in Boiling Water Reactors (BWR). Accurate neutron fluence determinations are required for a number of reasons: 1) to determine neutron fluence within the reactor pressure vessel (RPV) and at surveillance capsule locations to address vessel embrittlement issues; 2) to determine neutron fluence on the core shroud in order to determine fracture toughness and crack growth rate for use in flaw evaluation calculations; and 3) to determine neutron fluence at other internal components for structural integrity assessments or to evaluate repair technologies.

EPRI, under the direction of the BWR Vessel and Internals Project (BWRVIP) has developed the RAMA Fluence Methodology for predicting fluence in a manner that meets the NRC requirements. Fluence predictions are potentially required at many components within the reactor. However, there is a near term need for fluence calculations at surveillance capsule locations, within the vessel wall and the core shroud at elevations within the height of the active fuel. These "Priority 1" locations are addressed by the current methodology. In the future, the BWRVIP intends to extend the methodology for applicability to other internal components that are outside the elevation of the active core height.

1.2 Scope

The current methodology described herein predicts neutron fluence at all Priority 1 locations. The methodology includes computerized analysis tools to perform the fluence calculations, modeling guidelines describing the use of the methodology, and benchmark reports that document the capability of the methodology to predict neutron fluence.

The methodology includes a neutron transport code that is capable of accurately representing the reactor geometry and performing neutron flux calculations in true three-dimensional geometry, a nuclear data library which contains cross-section data and activation response factors which are suitable for neutron fluence determinations in BWR plants, and auxiliary processing codes to facilitate building detailed analysis models and determining dosimeter activities, neutron fluence, and uncertainties. The methodology adheres to the requirements set forth in NRC Regulatory Guide 1.190 [1] for pressure vessel neutron fluence determinations. This has been demonstrated by validating the methodology against specific benchmark problems identified in the regulatory guide and performing a plant-specific analysis.

The system of analysis tools developed for the BWR fluence methodology is provided in a software package referred to as the "RAMA Fluence Methodology". The RAMA Fluence Methodology includes the transport code that performs neutron transport calculations, the nuclear data library, and three supporting codes that were initially developed by TransWare Enterprises, Inc.: the RAFTER code that performs activation and uncertainty calculations, and the Parts Model Builder (PMB) and State-point Model Builder (SMB) codes that automate the process of preparing detailed computer models for the RAMA transport code.

1.3 Critical Characteristics

The RAMA Fluence Methodology performs fluence calculations for BWR Priority 1 components in a manner that meets Regulatory Guide 1.190. Following is a summary of key features and capabilities of the RAMA Fluence Methodology:

- Three-dimensional, multi-group transport code for calculating neutron flux. The transport methodology includes the capability to determine neutron source terms from input isotopic data and an anisotropic scattering treatment that is important for handling neutron transport from the in-core regions to the ex-core regions.
- Nuclear data that conforms to the cross sections and activation response functions contained in the industry standard BUGLE-96 nuclear data library [2].
- Accurate modeling and prediction of neutron fluence in the following specific BWR Priority 1 components: surveillance capsules, the reactor pressure vessel over the active fuel height (including axial and azimuthal profiles), and the core shroud over the active fuel height (including axial and azimuthal profiles).
- Capability to calculate dosimeter activation rates and to apply fluence trending evaluations, uncertainty, and bias adjustments identified in Regulatory Guide 1.190.
- Geometry and material model building tools to assist the user in constructing detailed reactor models.

1.4 Documentation

The following reports describe the RAMA Fluence Methodology software:

A Theory Manual (this report) describes the technical basis for the methodologies implemented in the RAMA computer codes. The Theory Manual also includes the technical basis for the methodologies used to generate the nuclear data library.

A User's Manual describes the installation, user interface, and input data requirements of the RAMA computer codes. The User's Manual also includes user information for the nuclear data library.

A Procedures Manual provides guidelines for the use of the methodology to perform neutron fluence, uncertainty and bias calculations in BWR Priority 1 components. The Procedures Manual also contains example problems that illustrate the process for building reactor models and performing fluence calculations.

A Benchmark Manual describes the benchmark problems and results. These benchmark problems provide an assessment of the accuracy and capabilities of the RAMA Fluence Methodology.

1.5 Requisite Skills

The RAMA Fluence Methodology is a technical tool that requires an understanding of reactor physics, computer modeling techniques, nuclear plant operation, fluence determinations, and uncertainty and bias determinations. The user of the software should have sufficient knowledge and experience in these technical areas in order to apply the software package correctly and to interpret the results generated by the software package. In general, the user should have a minimum Bachelor of Science degree in Nuclear Engineering or a related discipline.

1.6 Quality Assurance

The RAMA Fluence Methodology has been developed in accordance with 10CFR50 Appendix B and 10CFR21 requirements.

1.7 Target Platforms

The computer codes in the RAMA Fluence Methodology are written in conformance with the ISO/IEC Standard Fortran 95 [3] and ANSI Standard C [4] programming languages. Therefore, the software can be installed on any computer system supporting standard Fortran 95 and C compilers.

For this Project, the RAMA software shall be developed and maintained on desktop workstations employing Intel microprocessors and running the Linux operating system.

1.8 Document Organization

The remaining sections of this document describe the methodologies employed by the components of the RAMA Fluence Methodology to determine neutron fluence.

Section 2 provides an overview of the program architecture. A flow diagram illustrates how the code components work together and what data inputs are required.

Section 3 describes the geometry models employed in the transport code.

Sections 4-7 describe the methods used by RAMA, including the PMB, SMB, and RAFTER modules, respectively.

Section 8 describes the methods used to generate the nuclear data library.

Section 9 contains the references used in this document.

2
OVERVIEW OF PROGRAM ARCHITECTURE

This section provides a brief description of the RAMA Fluence Methodology software architecture and logic flow.

The software is designed to perform neutron and gamma ray flux calculations, determine neutron fluence, and calculate nuclide activation for BWR nuclear reactor assemblies. Each component of the software package is implemented to execute as a stand-alone program module. A top-level flow diagram of the software package is presented in Figure 2-1.

As Figure 2-1 shows, input to the software system comes from mechanical design drawing information and plant operating history data. The PMB tool processes the mechanical design inputs and generates the geometry information to build the geometry model for the desired component. The geometry data file generated by the PMB is then input into the transport code module.

The plant operating data is collected by the utility. Each utility has its own database for storing data. The utility generates a data file in a compatible format that will link with the SMB tool. The SMB tool processes the operating data and generates a material composition data file for input to the transport code. RAMA retrieves the geometry and material data, accesses nuclide cross section data from the nuclear data library and performs the neutron and gamma-ray flux calculations.

During the performance of a flux calculation, RAMA generates two additional files that provide data for subsequent executions of the same (or nearly the same) component geometry and state-point condition. These files are the Track Data File and the Flux Guess Data File. During an initial flux calculation, RAMA must convert the geometry and material information provided by the model builder tools, using ray tracing methods, to a format that can be used by the flux calculation. RAMA also uses standard flat flux guesses when performing an initial flux calculation. As a result of the initial flux calculation, RAMA generates a Track Data File that contains component geometry and material data in the form used directly by the flux calculation. It also generates a Flux Guess Data File that contains modified flux guesses generated specifically for that component during the flux calculation. These files allow RAMA to execute much faster when running a restart case because they provide data that was calculated in a previous run and does not need to be re-calculated in the present run.

During code execution, RAMA generates output list and ASCII data files containing the flux and dose rate data. The ASCII data files are retrieved by the RAFTER module for use in performing neutron fluence calculations. RAFTER also uses the plant operating history data for given state-points and dosimeter activity measurements to determine nuclide activation rates. The uncertainty methodology in RAFTER then adjusts the neutron fluence determination to provide an accurate neutron fluence for the given reactor component.

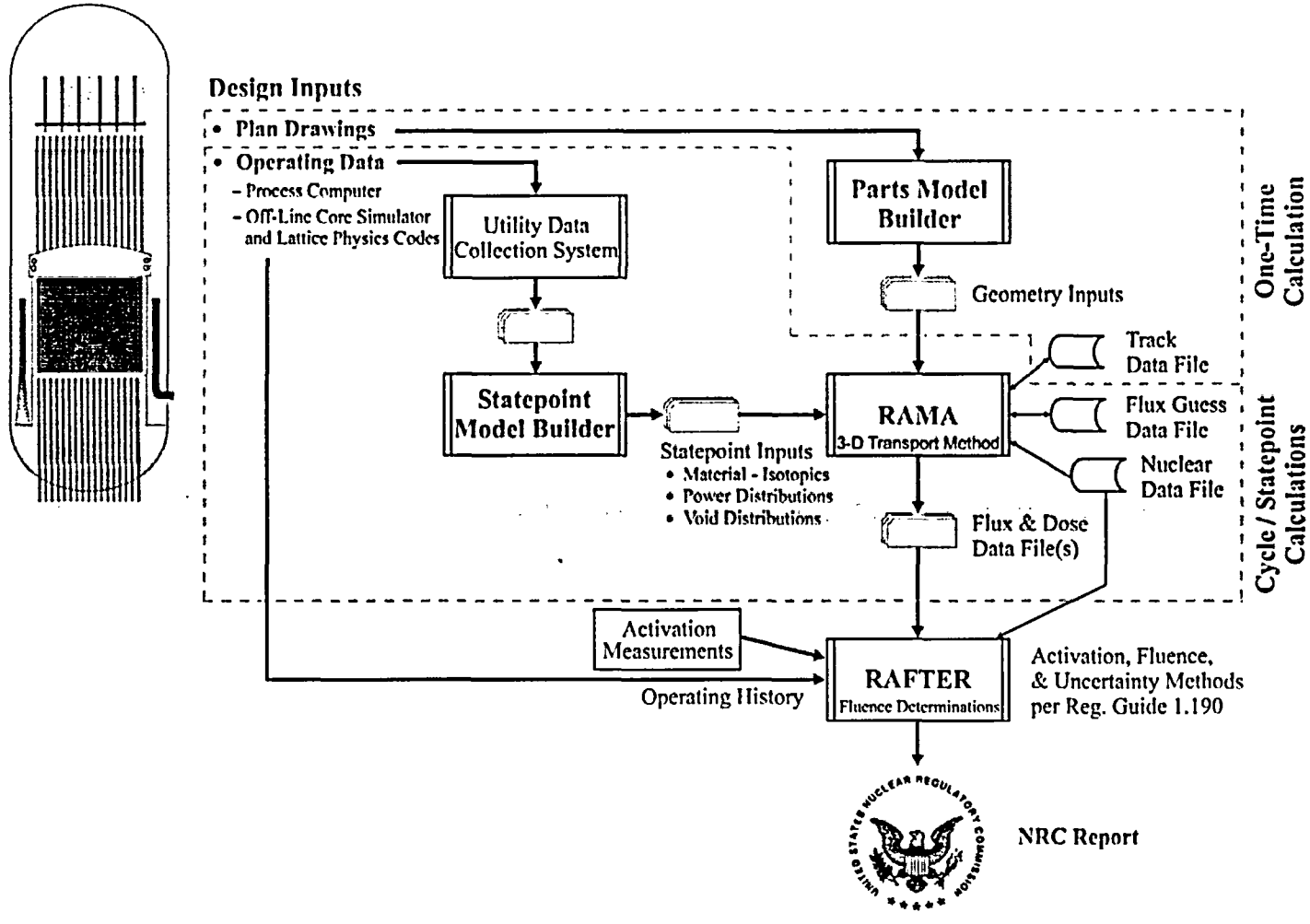

Figure 2-1
RAMA Fluence Methodology Software Architecture Flow Diagram

[This page intentionally left blank]

3
OVERVIEW OF GEOMETRY MODELING

This section provides an overview of the geometry modeling capabilities of the transport code. In essence, RAMA employs a geometry modeling capability that allows the user to describe the mechanical design of a reactor component at any desired level of modeling detail. To facilitate the use of the code, RAMA has a special input block that allows the user to easily describe very complex geometries with simple engineering inputs. The following subsections describe the geometry modeling method and provide examples of various parts models that are easily described using the geometry input data block. The User's Manual provides detailed descriptions for the geometry input data block.

3.1 Combinatorial Geometry Model

RAMA employs a combinatorial geometry modeling capability, similar to the methods used in Monte Carlo codes, that allows the user to describe problem geometries at any level of mechanical design detail. The geometry model is based on the combination of primitive geometry elements, e.g., rectangular parallelepipeds, right circular cylinders, right angle wedges, etc., to form geometry components having combinations of linear and curvilinear surfaces. A simple geometry component, or part, is described by a single geometry element. Complex geometry components, or parts, are described by specifying the differences and intersections of two or more primitive geometry elements. The primitive geometry elements most commonly used to describe geometry models are:

- arbitrary polyhedron,
- general box,
- ellipsoid,
- right angle wedge,
- right circular cylinder,
- right elliptical cylinder,
- rectangular parallelepiped,
- sphere, and
- truncated right angle cone.

The geometry model is similar in application to the combinatorial geometry techniques described in the MARS [5] geometry modeling system and used in various Monte Carlo codes such as SAM-CE [6]. The RAMA geometry model is very flexible. It allows the user to describe one or several unique individual parts in a local coordinate system. One or more instances of these parts are then placed in the proper absolute coordinates of the final solution geometry using positioning vectors. In restart cases, the user may easily replace any part in the solution geometry with another part using simple user input options.

The flexibility of the combinatorial geometry model can result in geometry descriptions that are very large and complex. To facilitate the use of the RAMA geometry modeling capability, RAMA supports an input data block that uses simple engineering data to describe the parts by dimensions, materials and meshing options. The code then automatically builds the parts descriptions in combinatorial geometry terms.

The following subsections describe the general geometry shapes used in RAMA to model any reactor component to detailed design descriptions. A discussion of how the Parts Model Builder combines these basic shapes to construct models of reactor components is provided in Sections 4 and 5. Additional information for building geometry models is provided in the User's Manual.

3.2 General Geometries

3.2.1 ARB - Arbitrary Convex Polyhedron

The arbitrary convex polyhedron body, "ARB", is a flexible geometry that can define 4, 5, and 6 sided bodies. A 6-sided arbitrary convex polyhedron body is illustrated in Figure 3-1.

The ARB body requires 30 values to describe the arbitrary convex polyhedron geometry. The first 8 sets of 3 values (24 values) define 8 vertices, $\vec{V}_1 - \vec{V}_8$, in (x, y, z) coordinates. These vertices are used to describe the shape and dimensions of the sides of the body. The remaining 6 values define the faces of the body. Each face is described by a 4-digit number, where each digit corresponds to an index of a vertex. For example, the value "1234" corresponds to the face defined by the vertices, $\vec{V}_1, \vec{V}_2, \vec{V}_3$, and $\vec{V}_4$. The faces may be specified in any order; however, the indexes for a face must be entered in either clockwise or counterclockwise order.

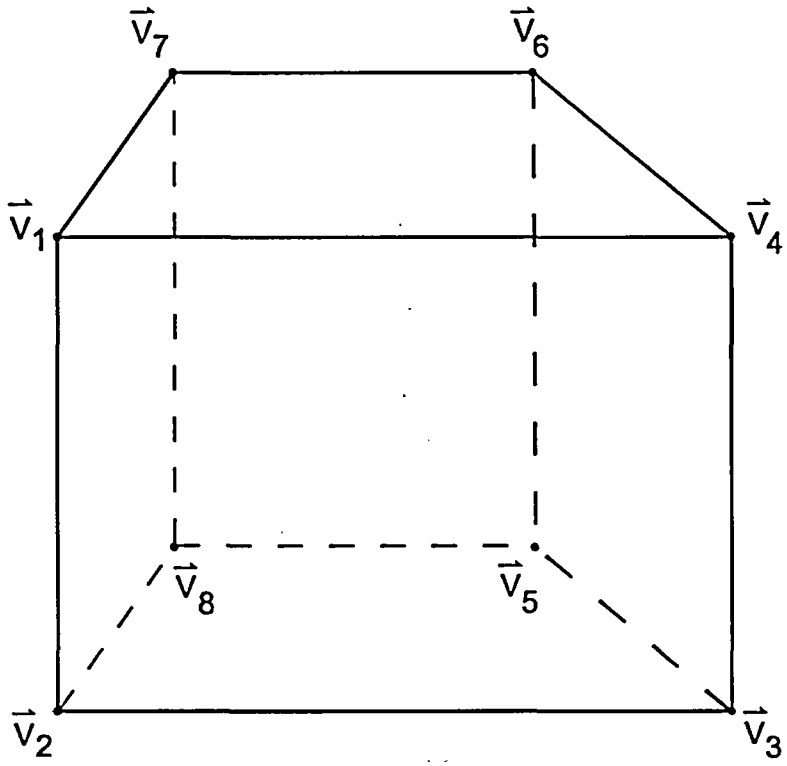

Figure 3-1
Arbitrary Convex Polyhedron Geometry

3.2.2 BOX - General Box

The general box body, "BOX", is a rectangular parallelepiped body that may be oriented arbitrarily relative to the coordinate axes. The general box body is illustrated in Figure 3-2.

The BOX body requires twelve values to describe the general box geometry. The first set of 3 values defines the origin of the body, (V_x, V_y, V_z). The following 3 sets of 3 values define mutually perpendicular sides of the body, (H_{1x}, H_{1y}, H_{1z}), (H_{2x}, H_{2y}, H_{2z}), and (H_{3x}, H_{3y}, H_{3z}) where, for example, the three components of H1 describe the length and orientation of H1 with respect to the coordinate system.

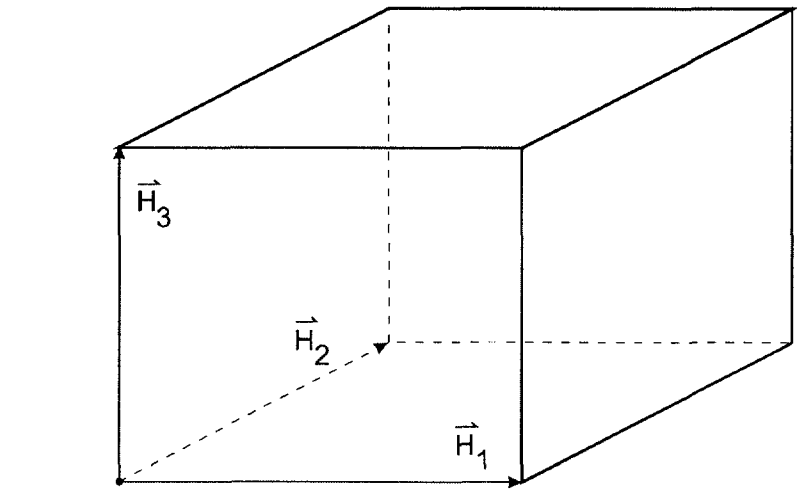

$\vec{V}\,(V_X, V_Y, V_Z)$

Figure 3-2
General Box Geometry

3.2.3 ELL - Ellipsoid

The ellipsoid body, "ELL", is illustrated in Figure 3-3. The ELL body requires seven values to describe the ellipsoid geometry. The first two sets of 3 values, $\vec{V}_1$ and $\vec{V}_2$ define the vertices of the foci in (x, y, z) coordinates. The last value is a scalar value, R, which defines the length of the major axis.

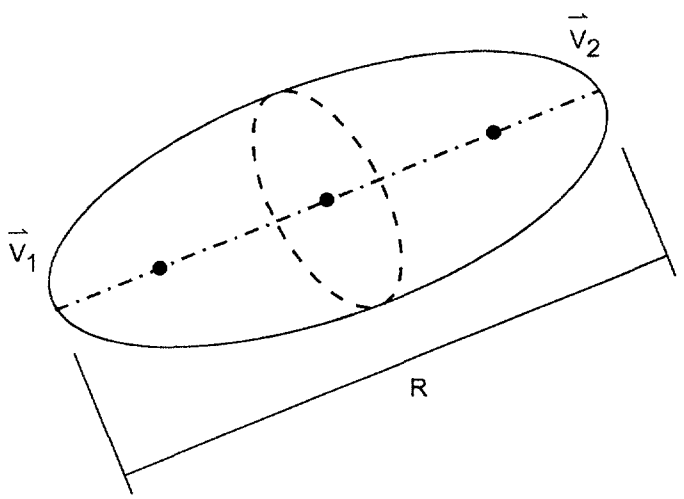

Figure 3-3
Ellipsoid Geometry

3.2.4 RAW - Right Angle Wedge

The right angle wedge body, "RAW", is illustrated in Figure 3-4. The RAW body requires twelve values to describe the right angle wedge geometry. The first set of 3 values defines the vertex of the RAW body, (V_x, V_y, V_z). The right angles that describe the faces of the wedge will be defined relative to the vertex point. The next two sets of 3 values define the vectors, (H_{1x}, H_{1y}, H_{1z}) and (H_{2x}, H_{2y}, H_{2z}), that describe the directions and dimensions for the sides of the body. The last set of 3 values defines a perpendicular vector, (B_x, B_y, B_z), that describes the height of the wedge body.

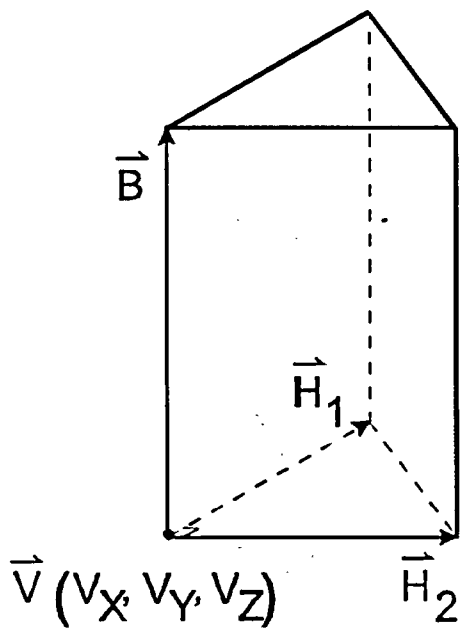

Figure 3-4
Right Angle Wedge Geometry

3.2.5 RCC - Right Circular Cylinder

The right circular cylinder body, "RCC", is illustrated in Figure 3-5. The RCC body requires seven values to describe the right circular cylinder geometry. The first set of 3 values, (V_X, V_Y, V_Z) defines the origin of the base plane of the cylinder. The second set of 3 values, (H_X, H_Y, H_Z) specifies the height and direction of the cylinder perpendicular to the base plane. The last value, R, defines the radius of the cylinder.

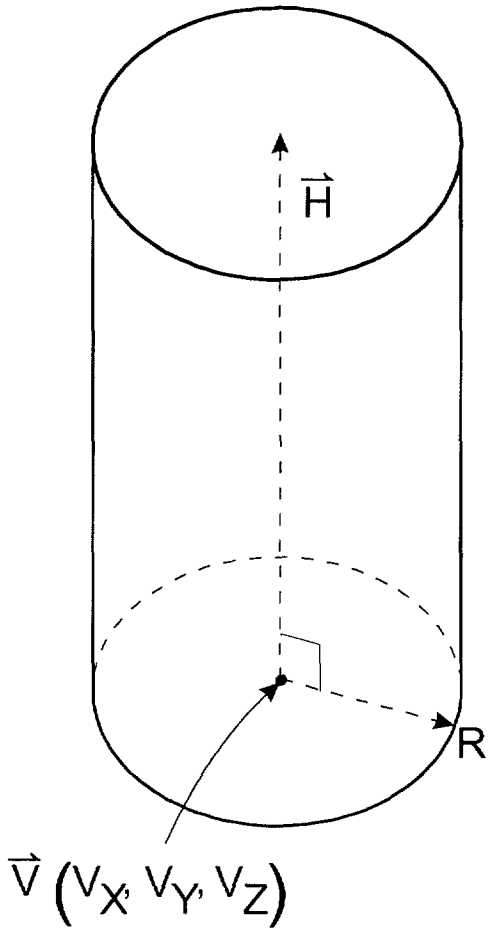

Figure 3-5
Right Circular Cylinder Geometry

3.2.6 REC - Right Elliptical Cylinder

The right elliptical cylinder body, "REC", is similar to an RCC body (see Section 3.2.5) except that the shape of the cylinder is elliptical instead of a circular. Figure 3-6 illustrates a REC body. The REC body requires twelve values to describe the right elliptical cylinder geometry. The first set of 3 values, (V_X, V_Y, V_Z), defines the center of the elliptical cylinder in the base plane. The second set of 3 values, (H_X, H_Y, H_Z), specifies the height and direction of the elliptical cylinder. The last two sets of 3 values, (R_{1x}, R_{1y}, R_{1z}) and (R_{2x}, R_{2y}, R_{2z}), define the direction and length of the major and minor axes of the elliptical cylinder.

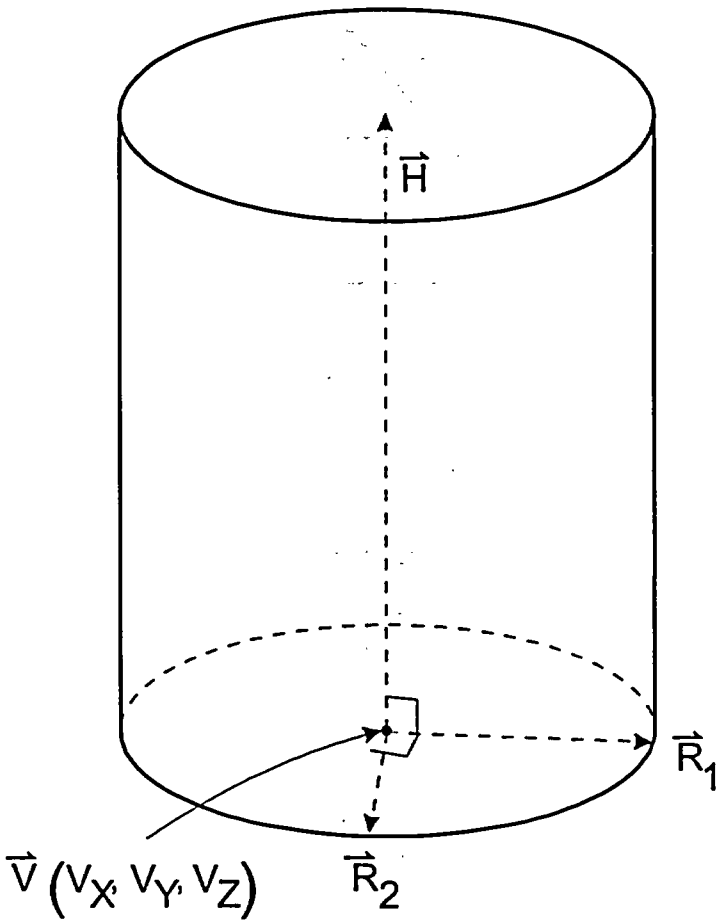

Figure 3-6
Right Elliptical Cylinder Geometry

3.2.7 RPP - Rectangular Parallelepiped

The rectangular parallelepiped body, "RPP", is similar to the BOX body (see Section 3.2.2) except the sides of the RPP body are parallel to the coordinate axes. The rectangular parallelepiped body is illustrated in Figure 3-7.

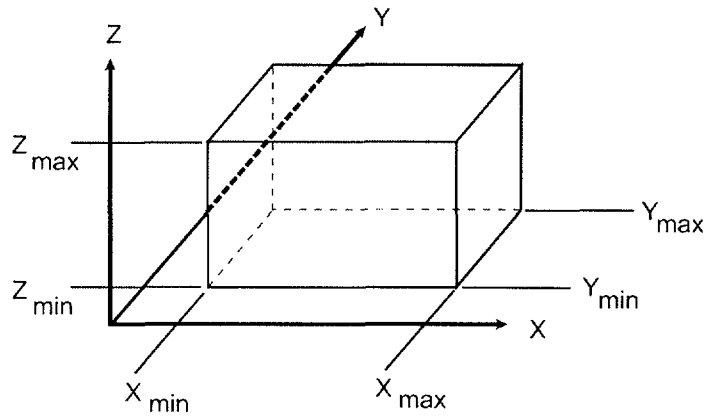

Figure 3-7
Rectangular Parallelepiped Geometry

The RPP body requires six values to describe the rectangular parallelepiped geometry. The first set of two values, X_{min} and X_{max}, define the minimum and maximum coordinates on the x-axis. The second set of two values, Y_{min} and Y_{max}, define the minimum and maximum coordinates on the y-axis. The third set of two values, Z_{min} and Z_{max}, define the minimum and maximum coordinates on the z-axis.

3.2.8 SPH - Sphere

The sphere body, "SPH", is illustrated in Figure 3-8. The SPH body requires four values to describe the sphere geometry. The first set of 3 values, (V_X, V_Y, V_Z), defines the centroid of the sphere. The fourth value, R, defines the radius of the sphere.

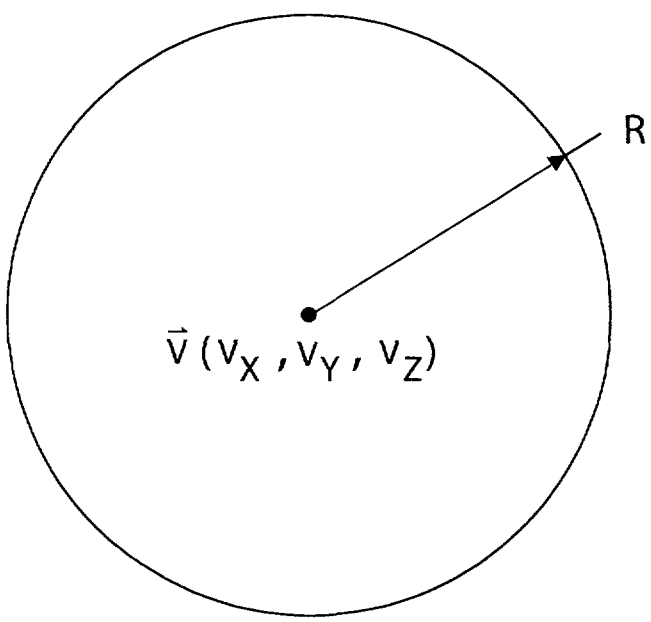

Figure 3-8
Sphere Geometry

3.2.9 TRC - Truncated Right Angle Cone

The truncated right angle cone body, "TRC", is illustrated in Figure 3-9. The TRC body requires eight values to describe the truncated right angle cone geometry. The first set of 3 values, (V_x, V_Y, V_Z), defines the centroid of the base plane of the cone. The second set of 3 values, (H_X, H_Y, H_Z), defines the height and direction of the cone. The seventh and eighth values, R_1 and R_2, define the lower and upper radii of the cone.

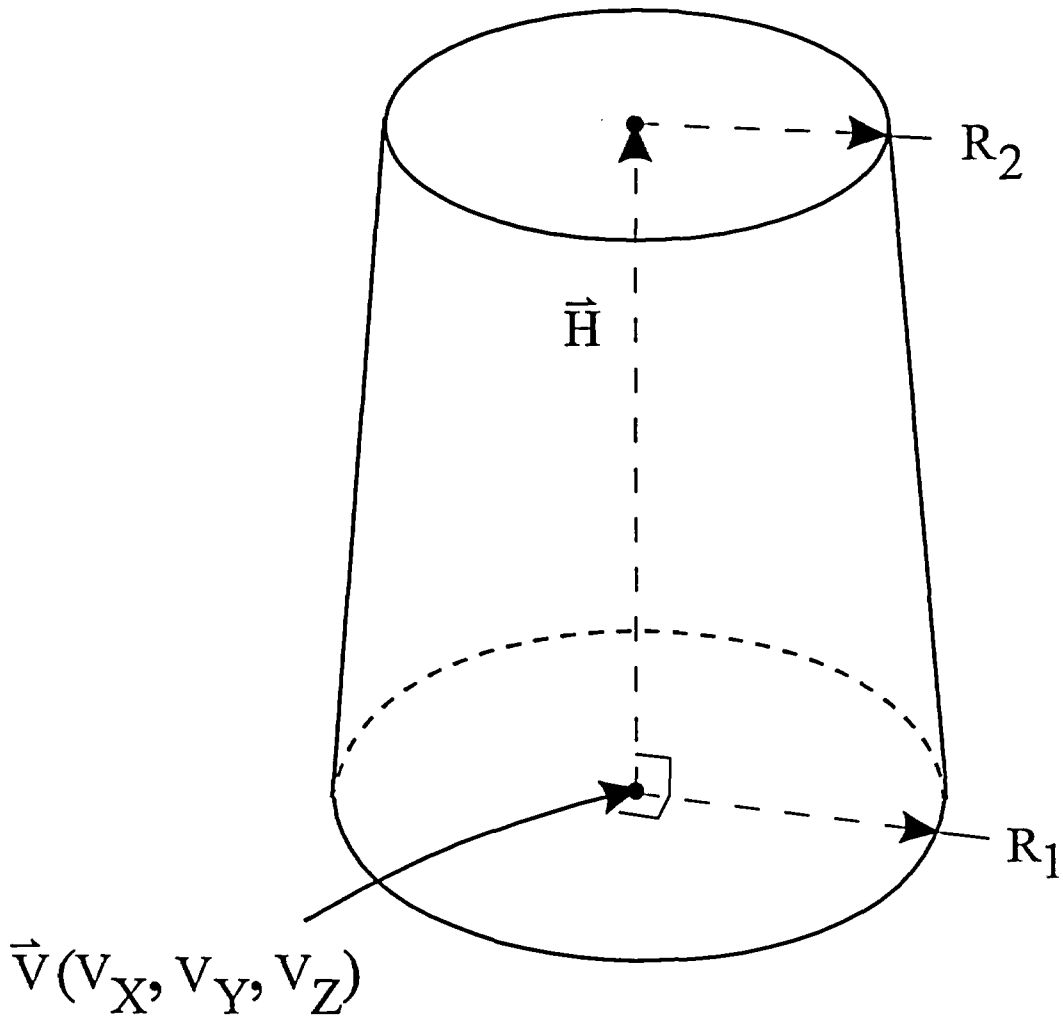

Figure 3-9
Truncated Right Angle Cone Geometry

[This page intentionally left blank]

4
TRANSPORT METHODS

This section describes the geometry models and solution methodologies that are employed by the RAMA transport code.

Section 4.1 describes the geometry modeling capabilities of the transport code. RAMA employs a geometry modeling technique that allows the user to model virtually any geometry problem in true three-dimensional detail.

Section 4.2 describes the nuclear transport methods used to solve the neutron and gamma-ray flux distribution problems. The transport theory is based upon the method of characteristics. The unique methods implemented in the code include treatments for three-dimensional spatial flux calculations and anisotropic scattering.

4.1 Geometry

RAMA employs a geometry modeling capability that is based upon combinatorial geometry techniques, similar to those in many Monte Carlo transport codes. This capability allows the user to describe virtually all parts of a reactor assembly in true three-dimensional design detail. This section describes the geometry coordinate system for a typical Boiling Water Reactor (BWR) assembly.

4.1.1 Coordinate System

Figure 4-1 illustrates the absolute coordinate system for a BWR reactor assembly model. RAMA uses the Cartesian coordinate system to describe the orientation of the reactor pressure vessel in space. The origin of the coordinate system is located on the inner surface of the vessel wall and is centered at the bottom drain plug. The z-axis is oriented along the vertical axis of the vessel. The xy-plane is perpendicular to the z-plane.

Individual reactor assembly parts may be described in a local Cartesian coordinate system for the modeling convenience of the user. The local coordinate system must then be defined such that the parts can be moved into the absolute coordinate system using simple positional vectors.

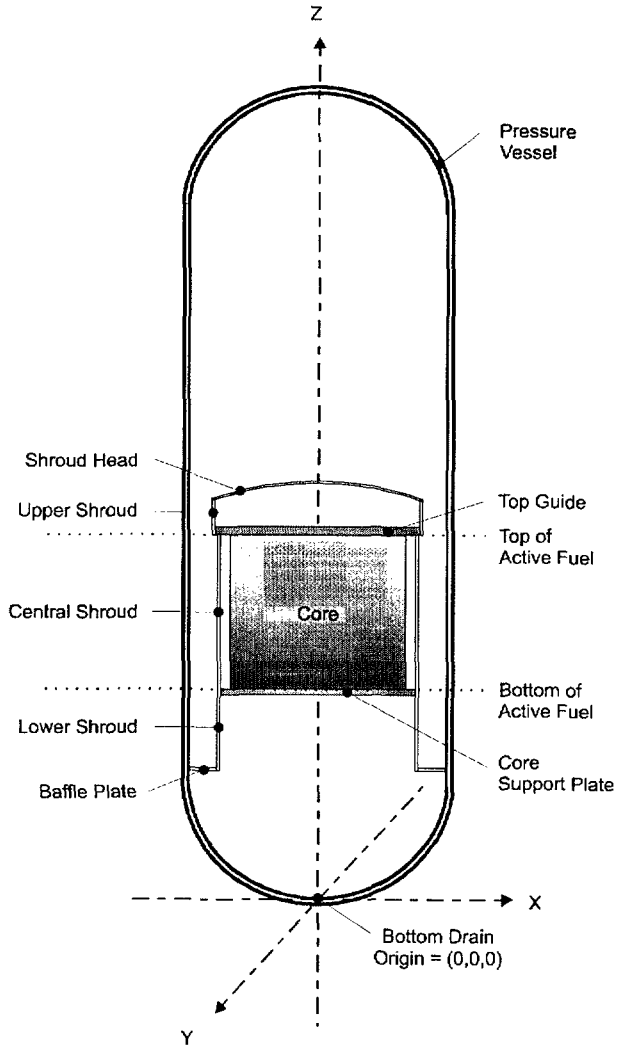

Figure 4-1
BWR Reactor Assembly Coordinate System

4.1.2 Reactor Models

The RAMA transport code is used to model the BWR system to calculate neutron flux. For modeling convenience, the BWR system is described in three axial zones. The first zone is comprised of the reactor core, pressure vessel components and coolant regions that lie between the axial elevations defined as the bottom of active fuel and top of active fuel. The second zone is comprised of the pressure vessel components and coolant regions that lie above the top of active fuel and the third zone is comprised of all components and coolant regions that lie below the bottom of active fuel. Figure 4-2 illustrates the three axial zones used in the RAMA models.

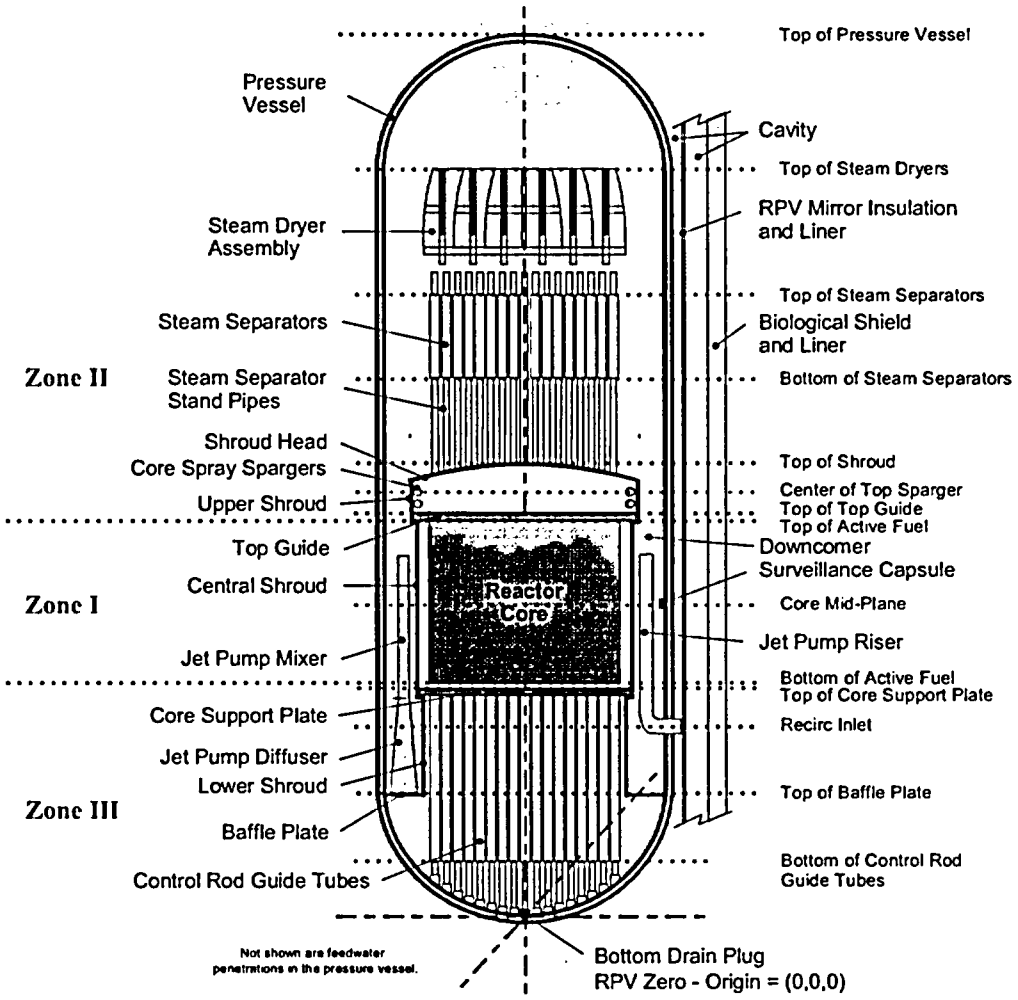

Figure 4-2
Cutaway View of a BWR Pressure Vessel Showing the Axial Zones

The Priority 1 components of interest in BWRs are all located within Zone 1. The major Priority 1 components and regions that must be represented in the RAMA transport calculation include the reactor core, central shroud, central downcomer, jet pump assemblies, dosimetry / surveillance capsules, and pressure vessel. The BWR Priority 1 model may also include representations for the pressure vessel mirror insulation, cavity, and biological shield (concrete wall), as required, to provide radial boundary conditions for the neutron transport calculation.

4.1.2.1 Combinatorial Geometry Models

RAMA employs a geometry modeling capability that allows the user to describe any part in the reactor assembly in true mechanical design detail. Accurate representations of straight and curved surfaces at any orientation are supported. The geometry model is coupled with a ray-tracing method that allows the code to determine accurate transmission probabilities of neutron and gamma-ray particles through material regions.

RAMA's geometry modeling capability is based upon three-dimensional combinatorial geometry techniques. The geometry modeling capability supports appropriate ray-tracing calculation methods to permit interfacing with the nuclear transport theory methods.

4.1.2.2 Geometry Symmetry

RAMA supports the capability to model problem geometries of any symmetrical form, thus allowing a reduced model for calculations.

4.1.2.3 Meshing

The geometry modeling capability allows parts to be described by one or more sub-volumes for purposes of meshing the problem.

4.1.3 Material Descriptions

RAMA has the capability to assign materials to all regions of the problem geometry. Material regions are described with the following attributes:

- Material type (e.g., SS304),
- Nuclides and nuclide concentrations in atoms/barn-cm, and
- Relative power term of the material in the material region.

4.2 Flux Calculation Methods

4.2.1 Particle Transport Equation

The basic equation that describes neutron transport is the Boltzmann equation [7]. The steady state form of this equation can be expressed as

$$\bar{\Omega} \cdot \nabla \psi(\bar{r},\bar{\Omega},E) + \Sigma'(\bar{r},E)\psi(\bar{r},\bar{\Omega},E) = q(\bar{r},\bar{\Omega},E) \tag{4-1}$$

with

$$q(\bar{r},\bar{\Omega},E) = \int\int \Sigma^{s}(\bar{r};\bar{\Omega}',E' \rightarrow \bar{\Omega},E)\psi(\bar{r},\bar{\Omega}',E')d\bar{\Omega}'dE' + Q(\bar{r},\bar{\Omega},E) \tag{4-2}$$

where $\psi(\bar{r},\bar{\Omega},E)$ is the angular flux in the $\bar{\Omega}$ direction at location $\bar{r}$ with energy E, $\Sigma'(\bar{r},E)$ is the total interaction cross-section at location $\bar{r}$ with energy E, $\Sigma^{s}(\bar{r};\bar{\Omega}',E' \rightarrow \bar{\Omega},E)$ is the cross-section at location $\bar{r}$ for scattering from direction $\bar{\Omega}'$ with energy E' to direction $\bar{\Omega}$ with energy

E, and $Q(\bar{r},\bar{\Omega},E)$ is the neutron or gamma, as appropriate, source at location $\bar{r}$ in the $\bar{\Omega}$ direction with energy E.

Equation (4-1) is a first order differential equation that forms the basis for determining the angular particle densities in a general geometry system. (Note that technically, Equation (4-1) is an integro-differential equation, since the RHS contains an integral scattering source term.) A discrete solution of Equation (4-1) can be obtained by any of several means. Historically, discrete ordinates methods [7] have been utilized to solve the angular particle transport equation for regular mesh geometry problems. Unfortunately, discrete ordinates methods are not well suited to combinatorial geometry modeling and require fine geometry meshing due to the loose coupling of the various meshed solution regions. For applications that require general geometry modeling capabilities, it is desirable to solve Equation (4-1) by means of a more robust solution technique, such as the method of characteristics solution methodology used in RAMA.

4.2.2 Characteristics Solution Methodology with Anisotropic Scattering

A formulation of the Boltzmann equation that is suited to problems with a large number of solution regions (i.e., greater than a few hundred solution regions) has been developed utilizing an implementation that is similar to a characteristic solution methodology which preserves the angular dependence of the transport equation in three-dimensional geometry.

Equation (4-1) can be simplified by noting that all of the streaming must occur along the $\bar{\Omega}$ direction; thus the first term can be expressed as a directional derivative in direction $\bar{\Omega}$. Defining the position vector in terms of distance, s, along the $\bar{\Omega}$ vector such that $\bar{r} = \bar{r}_0 + s\bar{\Omega}$ leads to the simplification

$$\bar{\Omega} \cdot \nabla \psi \rightarrow \frac{d}{ds}\psi(\bar{r}_0 + s\bar{\Omega},\bar{\Omega},E) \tag{4-3}$$

where r_0 is a reference point (usually chosen on the outer boundary) for the origin of a ray in the direction of $\bar{\Omega}$. This allows Equation (4-1) to be written as

$$\frac{d}{ds}\psi(\bar{r}_0 + s\bar{\Omega},\bar{\Omega},E) = \Sigma'(\bar{r}_0 + s\bar{\Omega},E)\psi(\bar{r}_0 + s\bar{\Omega},\bar{\Omega},E) = q(\bar{r}_0 + s\bar{\Omega},\bar{\Omega},E) \tag{4-4}$$

The derivation of the characteristic solution methodology consists of integrating the basic transport equation presented in Equation (4-4) along rays (i.e., straight lines) in the characteristic direction $\bar{\Omega}$ with distance along the ray denoted by the variable s. It is convenient to consider the application of Equation 4-4 to any ray passing through a volume, V_i, where the volume is sufficiently small that the material properties are constant throughout the volume (i.e., the cross sections do not vary spatially within the volume) and the distance variable, s, is considered to be measured relative to the entry point of the ray in the volume. The differential equation that defines the angular flux along any such ray within volume V_i can be written as:

$$\frac{d}{ds}\psi_i(s,\bar{\Omega},E)+\Sigma_i^t(\bar{\Omega},E)\psi_i(s,\bar{\Omega},E)=q(s,\bar{\Omega},E) \tag{4-5}$$

where the source term in Equation (4-5) can be expressed as:

$$q_i(s,\bar{\Omega},E)=\iint\Sigma_i^s(\bar{\Omega}',E'\rightarrow\bar{\Omega},E)\psi_i(s,\bar{\Omega}',E')d\bar{\Omega}'dE'+Q(s,\bar{\Omega},E) \tag{4-6}$$

At this point it is convenient to convert Equations (4-5) and (4-6) into a form that consists of a discrete set of angular directions and energy groups. Letting the discrete form of the angular flux be defined as:

$$\Phi_{i,k,g}(s)\equiv\int_{\Delta E_g}\int_{\Delta\Omega_k}\psi_i(s,\bar{\Omega},E)d\bar{\Omega}\,dE \tag{4-7}$$

where ΔE_g is the energy range corresponding to energy group g and $\Delta\Omega_k$ is a differential solid angle about direction $\bar{\Omega}_k$.

Integrating both sides of Equation (4-5) over the discrete solid angle $\Delta\Omega_k$ and the discrete energy group range ΔE_g, and assuming that the nuclear cross sections at any location are constant within the differential solid angle and energy group, yields:

$$\frac{d}{ds}\int_{\Delta E_g}\int_{\Delta\Omega_k}\psi_i(s,\bar{\Omega},E)d\bar{\Omega}\,dE+\Sigma_{i,g}^t\int_{\Delta E_g}\int_{\Delta\Omega_k}\psi_i(s,\bar{\Omega},E)d\bar{\Omega}\,dE=\int_{\Delta E_g}\int_{\Delta\Omega_k}q_i(s,\bar{\Omega},E)d\bar{\Omega}\,dE \tag{4-8}$$

where $\Sigma_{i,k,g}^t$ is the total interaction cross section in the differential solid angle $\Delta\Omega_k$ and energy group range ΔE_g. Using the definition in Equation (4-7), Equation (4-8) can be expressed as:

$$\frac{d}{ds}\Phi_{i,k,g}(s)+\Sigma_{i,g}^t\Phi_{i,k,g}(s)=q_{i,k,g}(s) \tag{4-9}$$

The source term in Equation (4-9) can be determined by substituting Equation (4-6) into Equation (4-8) to yield:

$$q_{i,k,g}(s)=\int_{\Delta\Omega_k}d\bar{\Omega}\sum_{g'=1}^{G}\sum_{k'=1}^{K}\Sigma_{i,k'\rightarrow k,g'\rightarrow g}^{s'}\Phi_{i,k',g'}(s)+\int_{\Delta E_g}\int_{\Delta\Omega_k}Q_i(s,\bar{\Omega},E)d\bar{\Omega}\,dE \tag{4-10}$$

where $\Sigma_{i,k'\rightarrow k,g'\rightarrow g}^{s'}$ is the anisotropic scattering cross section for scattering from discrete angle k′ to discrete angle k and from energy group g′ to energy group g, and the integrals over all energy and all angular directions have been replaced by summations over the number of discrete angles (K) and the number of energy groups (G).

The anisotropic scattering cross section in Equation (4-10) can be represented by a partial expansion of Legendre polynomials [7]. Letting

$$\Sigma^{s}_{i,k'\to k,g'\to g} \approx \sum_{m=0}^{M} (2m+1)\Sigma^{(m)}_{i,g'\to g} P^{(m)}\left(\mu_{k'\to k}\right) \tag{4-11}$$

allows the anisotropic scattering term to be written as:

$$\Sigma^{s'}_{i,k'\to k,g'\to g} = \frac{\Sigma^{s'}_{i,k'\to k,g'\to g}}{4\pi} \tag{4-12}$$

where $\Sigma^{(m)}_{i,g'\to g}$ is the m-th order scattering moment from energy group g' to energy group g, $P^{(m)}$ is the m-th order Legendre polynomial and $\mu_{k'\to k}$ is the cosine of the angle between $\bar{\Omega}_{k'}$ and $\bar{\Omega}_{k}$ that is

$$\mu_{k'\to k} = \bar{\Omega}_{k'} \cdot \bar{\Omega}_{k} \tag{4-13}$$

If particle production is assumed to be from an isotropic source (e.g., neutron production from fissions) that is uniform throughout volume V_i, then the production term can be represented as:

$$\int_{\Delta\Omega_k} \int_{\Delta E_g} Q_i(s,\bar{\Omega},E)\,dE\,d\bar{\Omega} = Q_{i,g} \frac{\int_{\Delta\Omega_k} d\bar{\Omega}}{4\pi} \tag{4-14}$$

where $Q_{i,g}$ is the uniform particle production rate in energy group g within volume V_i.

Substituting Equations (4-12) and (4-14) into Equations (4-9) and (4-10) results in the following expression for the angular flux in volume V_i to be written in the form:

$$\frac{d\Phi_{i,k,g}(s)}{ds} + \Sigma_{i,k,g}\Phi_{i,k,g}(s) = \hat{q}_{i,k,g} \tag{4-15}$$

where

$$\Sigma_{i,k,g} = \Sigma^{t}_{i,g} - W_k \Sigma^{s}_{i,k,g} \tag{4-16}$$

$$\hat{q}_{i,k,g} = W_k \left(Q_{i,g} + \sum_{\substack{g'=1 \\ g',k'\neq g,k}}^{G} \sum_{k'=1}^{K} \Sigma^{s}_{i,k'\to k,g'\to g} \overline{\Phi}_{i,k',g'} \right) \tag{4-17}$$

and

$$W_k = \frac{\int_{\Delta\Omega_k} d\bar{\Omega}}{4\pi} = \frac{\Delta\Omega_k}{4\pi} \tag{4-18}$$

Equation (4-17) has been made a constant along the entire length of the ray within volume V_i by approximating the angular flux values in all angular directions except the $\bar{\Omega}_k$ direction by the average angular flux in volume V_i. As a result, at a given solution iteration the particle angular flux contributions to the source term in Equation (4-17) are held constant. Under this assumption, the average particle angular flux along a given ray in the $\bar{\Omega}_k$ direction can be determined by direct integration of Equation (4-15) to yield

$$\overline{\Phi}^r_{i,k,g} = \frac{\Phi^{I,r}_{i,k,g} - \frac{\hat{q}_{i,k,g}}{\Sigma_{i,k,g}}}{\tau^r_{i,k,g}}\left(1 - e^{-\tau^r_{i,k,g}}\right) + \frac{\hat{q}_{i,k,g}}{\Sigma_{i,k,g}} \tag{4-19}$$

where $\Phi^{I,r}_{i,k,g}$ is the value of the angular flux along ray r at the entrant boundary and $\tau^r_{i,k,g}$ is the optical distance through volume V_i for a particle traveling along ray r in energy group g, as given by:

$$\tau^r_{i,k,g} \equiv \Sigma_{i,k,g} d^r_i \tag{4-20}$$

where d^r_i is the distance through volume V_i.

Now consider the situation wherein more than one parallel ray traverses volume V_i in the $\bar{\Omega}_k$ direction. Because the flux physically corresponds to the track length within the volume, the total average angular flux in volume V_i in the $\bar{\Omega}_k$ direction in energy group g can be expressed as the volume weighted contribution of the incremental average flux values from each ray, such that

$$\overline{\Phi}_{i,k,g} = \frac{\sum_{r=1}^{R} \overline{\Phi}^r_{i,k,g} \Delta V_r}{\sum_{r=1}^{R} \Delta V_r} \tag{4-21}$$

where R is the total number of parallel rays through volume V_i, and the differential volume subtended by ray r as it traverses the volume, denoted by ΔV_r is given by

$$\Delta V_r = d^r_i \Delta A_r \tag{4-22}$$

where ΔA_r is the cross-sectional area subtended by ray r. The scalar flux can be determined from Equation (4-21) to be:

$$\phi_{i,g} = \sum_{k=1}^{K} \overline{\Phi}_{i,k,g} \tag{4-23}$$

The value of the angular flux at the exit boundary of volume V_i, along ray r, denoted by $\Phi^{0,r}_{i,k,g}$ can also be determined from the solution of Equation (4-15) to be:

$$\Phi^{0,r}_{i,k,g} = \left(\Phi^{I,r}_{i,k,g} - \frac{\hat{q}_{i,k,g}}{\Sigma_{i,k,g}} \right) e^{\tau^{r}_{i,k,g}} + \frac{\hat{q}_{i,k,g}}{\Sigma_{i,k,g}} \tag{4-24}$$

Note that this value is also the value of the angular flux at the entrant boundary of the volume adjacent to volume V_i along a given ray.

4.2.2.1 Ray Tracing Methodology

The application of the characteristic solution methodology described in Section 4.2.2, consists of saturating the solution geometry with sets of parallel rays that are projected through the geometry in various directions defined by an angular quadrature set. The rays provide the characteristic directions along which integration of the particle angular flux is determined. Individual parts of the geometry may be sub-meshed to form suitably sized solution volumes. The points of intersection of the various rays with the surface of each subvolume are identified by using routines similar to those used in Monte Carlo calculations. These intersections, along with the angular scattering relationship specified by the angular scattering equation, are used to determine particle interactions throughout the modeled geometry. By utilizing the Legendre expansion form of the scattering cross-section, defined in Equation (4-11), the angular dependence of scattering source can be maintained in the solution process.

4.2.2.2 Neutron Source Due to Fissions

It is possible to utilize any known external particle source term in the solution process. However, a source of a special nature that deserves unique treatment is encountered when neutron transport in the vicinity of fission sources is being evaluated. In this case, the power distribution is typically known for external calculations, such as from three-dimensional nodal simulator codes. The corresponding neutron source terms must be determined by relating the fission source to the generated power in the fission regions.

In any operating reactor system, the source of neutrons can be assumed to be exclusively the result of the fission process in the core region. It is also reasonable to assume that the fission process emits neutrons isotropically. Under these assumptions, the neutron source term can be expressed in the form:

$$Q_{i,g} = p_i P_D \frac{\sum_{n=1}^{N_i} \chi_{n,g} \sum_{g'=1}^{G} \left(\nu\Sigma^f\right)_{n,g'} \phi_{i,g'}}{\sum_{g'=1}^{G} \sum_{n=1}^{N_i} \kappa_n^f \Sigma_{n,g'}^f \phi_{i,g'}} \tag{4-25}$$

where p_i is the relative power (normalized to a core volume average value of 1.0) in volume V_i, P_D is the power density (watts/cm^3) in the core region, $\chi_{n,g}$ is the fraction of neutrons emitted into energy group g from a fission of nuclide n, $\left(\nu\Sigma^f\right)_{n,g'}$ is the fission production cross section for nuclide n in energy group g', κ_n is the energy produced from a fission of nuclide n (joules/fission), $\Sigma_{n,g'}^f$ is the fission cross section of nuclide n in energy group g', and N_i is the total number of fissioning nuclides in volume V_i.

The transport solution assumes an initial scalar flux distribution, which, from Equation (4-25) provides an estimate of the actual neutron fission source distribution. This distribution, in turn, produces an updated scalar neutron flux. The resulting scalar neutron flux provides an improved estimate of the fission source term. The outer iteration process is continued until acceptable accuracy is obtained.

4.2.2.3 Boundary Condition Calculation

Two boundary conditions are treated in the method of characteristics solution methodology: vacuum boundaries and reflective boundaries.

Vacuum boundaries are quite easy to incorporate into the method of characteristics solution. By definition, there is no entering particle current at a vacuum boundary. As a result, there can be no entering angular flux for any ray that emanates from a vacuum boundary. In a method of characteristics solution process, this condition is equivalent to using an entrant angular flux value of zero (i.e., $\Phi_{1,k,g}^{l,r} = 0$).

Reflective boundaries are handled by reflecting each ray that emanates from a reflective boundary back into the body. The process is repeated at each reflective boundary of the problem until the total number of mean free paths measured from the entrant reflective surface exceeds a user defined maximum value.

The entrant angular flux at the start of a ray that emanates from a reflective boundary can be determined by noting that an alternative solution to the method of characteristics governing equation, i.e., Equation (4-4), can be written as the integral transport expression [7]:

$$\Phi\left(\bar{r},\bar{\Omega},E\right) = \int_0^{\infty} e^{-\int_0^{s'} \Sigma\left(\bar{r}-s''\bar{\Omega},E\right)ds''} q\left(\bar{r} - s'\bar{\Omega},\bar{\Omega},E\right)ds' \tag{4-26}$$

The corresponding angular flux at the entrant to the volume Vi can be expressed as:

Content Deleted -
EPRI Proprietary Information

where the subscripts denote successive regions encountered along the reflected portion of the ray, starting at the reflective boundary and progressing backward until the accumulated optical distance is greater than a user-defined maximum value.

4.2.3 Flux Edits Methods

Most reactor system component damage assessments are based upon flux values that are greater than a cutoff energy level, e.g., ϕ(E>1 MeV). If the energy cutoff value falls on a group boundary, the resulting flux that is greater than the energy cutoff value is simply the sum of the fluxes in the energy groups with lower energy range values that are above the cutoff value. In this case, the resulting neutron flux is given by:

$$\phi_{E_0} = \sum_{g \le G} \phi_g \tag{4-28}$$

where ϕ_{E_0} is the total flux with energy greater than the cutoff energy E_0, G is the energy group whose lower boundary value coincides with the cutoff energy value, g is the group index, and ϕ_g is the neutron flux in energy group g.

If the cutoff energy value does not coincide with a group boundary, then it is necessary to determine the contribution to the neutron flux from the energy group in which the cutoff energy value lies. In this case, the resulting neutron flux can be expressed as:

$$\phi_{E_0} = \sum_{g < G} \phi_g + \delta_G \tag{4-29}$$

where G is the energy group that the cutoff energy lies in and δ_G is the contribution from energy group G to the neutron flux that is greater than the cutoff energy.

Content Deleted -
EPRI Proprietary Information

(4-31)

(4-32)

Content Deleted -
EPRI Proprietary Information

(4-33)

(4-34)

5
GEOMETRY MODEL BUILDING METHOD

The RAMA transport code employs a geometry modeling capability that is based upon combinatorial geometry techniques. This capability allows the user to describe all parts of a reactor assembly in accurate three-dimensional design detail.

The Parts Model Builder (PMB) tool uses geometry elements to describe regions of the reactor. Nodal geometry modeling techniques are used when describing the reactor core region. Other regions of the reactor, such as the central shroud region or the downcomer region, are cylindrical in shape; therefore curvilinear geometry elements accurately describe these areas. Once a geometry element is selected to model a specific region, the PMB automatically regenerates these elements until the geometry model satisfies the dimensional specifications given by the user.

The PMB uses the basic geometry types described in Section 3.2 of this manual to generate geometries for the following parts and regions of a reactor model:

- fuel assemblies in the reactor core region;
- core reflector regions adjacent to, below, and above the reactor core region;
- the core shroud around the reactor core region;
- the downcomer region, including the jet pumps, between the core shroud and pressure vessel walls; and
- general cylindrical-shaped regions that include the pressure vessel, pressure vessel mirror insulation, cavity, and biological shield regions.

5.1 Generating the Reactor Core Region Geometry Model

The core geometry is described in (x,y)-coordinates. The fuel assembly locations are numbered beginning with (01,01) in the lower left corner of the geometry, and incrementing by +01 across the x-axis and +01 up the y-axis. The last region is in the upper right corner and has the value (NN,NN), where NN is the dimension of the reactor core.

The reactor core region is built using the fuel assembly descriptions input by the user. Fuel assembly parameters include assembly geometry type specifications, dimensions, and meshing options. Fuel assemblies are assumed to be square in the x-y plane and are built with the rectangular parallelepiped (RPP) bodies. The fuel assembly part may be specified as a nodal element corresponding to a fully-homogenized fuel assembly, or as sub-meshed elements corresponding to a supported fuel assembly geometry type.

5.1.1 Fuel Assembly Meshing and Volume Calculations

Fuel assembly meshing options range from pin-wise to fully homogenized. Fuel assemblies may be homogenized over the entire pitch of the fuel assembly region, or the fuel pins may be homogenized in the fuel bundle region preserving the channel and water gap regions around the fuel bundle that are present in BWR fuel assembly designs. Optionally, the fuel assemblies residing in the interior regions of the core may be modeled as a bulk region; thus, reducing the number of regions in the problem. A different mesh type may be specified for each fuel assembly location in the core region.

The volumes of fuel assemblies are calculated simply as length x width x height. Volumes for meshed fuel assemblies are calculated according to the mesh option used. Volumes for fuel assemblies that lie on symmetry lines are also calculated according to the symmetry of the region.

5.2 Generating the Core Reflector Region Geometry Model

The core reflector region is built in the radial plane beside the core region. The reflector region is bounded by the rectangular boundary of the core region and the curvilinear boundary of the core shroud. The parts generated by the PMB provide for the transition from rectangular to cylindrical form in the model. This is accomplished by intersecting rectangular parallelepiped (RPP) with right circular cylinder (RCC) bodies in the combinatorial geometry specification.

5.2.1 Core Reflector Meshing and Volume Calculations

Meshing of the core reflector parts is determined in three steps. First, a reflector part is built as a series of RPP regions, or sub-volumes, where each region has an equal volume in accordance with the meshing parameters specified by the user. Second, the RPP regions that are intersected by a RCC body are recalculated. Last, the regions affected by the RCC intersection are evaluated to determine if "extremely small" volumes result. If a small volume is formed, then the region with the small volume is joined with a neighboring region to form a larger volume. The region volumes are then re-evaluated to determine the acceptability of the meshing. If the joined region exceeds the meshing limits, the region is halved and the volumes are re-evaluated again. This process continues until acceptable volumes are attained for all mesh regions. Assuming that a nominal mesh region has the volume, V_{nom}, the following criteria are used to evaluate the acceptability of the calculated mesh volume, V_{mesh}:

Content Deleted -
EPRI Proprietary Information

5.3 Generating the Core Shroud Region Geometry Model

The core shroud is a cylindrical part in design and is built using RCC and right angle wedge (RAW) bodies. The RCC body provides the cylindrical shape and sub-annuli meshing of the shroud wall and the RAW body provides the sub-meshing of the circular parts to form arcs of equal azimuthal angle.

5.3.1 Shroud Meshing and Volume Calculations

The methods for determining the meshing in the shroud part are described in Section 5.6, *Radial and Azimuthal Meshing in Cylindrical Parts.*

5.4 Generating the Downcomer and Jet Pump Region Geometry Model

The downcomer water region is built in three radial zones. The inner zone lies in the annulus between the core shroud and jet pump assemblies, and spans all azimuthal angles in the problem geometry. The outer zone lies in the annulus between the jet pump assemblies and pressure vessel, and spans all azimuthal angles in the problem geometry. Both zones are formed from simple right circular cylinder (RCC) and right angle wedge (RAW) bodies.

The central zone lies in the annulus of the downcomer region between the inner and outer zones. It is constructed from two part types. The first part type is a column of arc meshes that spans the radial distance between the inner and outer zones. These parts are formed from simple right circular cylinder (RCC) and right angle wedge (RAW) bodies. The second part type is RCC bodies that describe the jet pump riser and mixer pipes and the water in the pipes. The method for calculating the meshing in these parts is described in Section 5.6.

5.4.1 Downcomer and Jet Pump Meshing and Volume Calculations

The methods for determining the meshing in the inner and outer zone regions of the downcomer are described in Section 5.6, *Radial and Azimuthal Meshing in Cylindrical Parts.*

Meshing in the central zone parts is determined in three steps. First, the meshing, or regions, for the part is determined using the technique described in Section 5.6 for right circular cylinders. Second, the regions are adjusted to account for the presence of the jet pump pipes. Last, the regions affected by the intersection of the jet pump pipes are evaluated to determine if "extremely small" volumes result. If a small volume is formed, then the region with the small volume is joined with a neighboring region to form a larger volume. The region volumes are then re-evaluated to determine the acceptability of the meshing. If the joined region exceeds the meshing limits, the region is halved and the volumes are re-evaluated again. This process continues until acceptable volumes are attained for all mesh regions. Assuming that a nominal mesh region has the volume, V_{nom}, the following criteria are used to evaluate the acceptability of the calculated mesh volume, V_{mesh}:

Content Deleted -
EPRI Proprietary Information

5.5 Generating Geometry Models Containing Pipe Elements

PMB uses pipe elements for certain geometry models. Typical components that use pipe elements include the reactor pressure vessel, pressure vessel mirror insulation, biological shield (concrete wall), and cavity region.

Pipe parts are circular in design and are built with RCC and RAW bodies. RCC bodies describe the inner and outer radii of the pipes. RCC bodies are also used to describe sub-annulus meshing in the pipe wall. The RAW body is used to sub-mesh the pipe wall into arcs of equal azimuthal angles.

5.5.1 Pipe Element Meshing and Volume Calculations

The methods for determining the meshing in pipe elements are described in Section 5.6, *Radial and Azimuthal Meshing in Cylindrical Parts.*

5.6 Radial and Azimuthal Meshing in Cylindrical Parts

The PMB code calculates radial and azimuthal meshing in cylindrical parts in accordance with meshing parameters specified by the user. The cylindrical parts are built using RCC bodies. The cylindrical parts are meshed into arcs using RAW bodies. The RCC body provides the cylindrical shape and radial meshing of the part and the RAW body provides the azimuthal meshing of the part.

Radial sub-meshing is accomplished by determining an appropriate number of RCC bodies in the circular part. Radial meshing may be determined using either the equal radius or equal volume method.

Radial meshing, ΔR, in the equal radii method is determined as:

$$\Delta R = \frac{R_{outer} - R_{inner}}{N} \tag{5-1}$$

where R_{outer} is the outer radius of the cylinder part, R_{inner} is the inner radius of the part, and N is the number of sub-annuli in the part.

Radial meshing in the equal volume method is determined in two steps. First, the volume per unit height of a mesh region, ΔV, is determined as:

$$\Delta V = \frac{\pi(R^2{}_{outer} - R^2{}_{inner})}{N} \tag{5-2}$$

The radii for the mesh volumes are then determined by consecutively adding the mesh volume, ΔV, to the volume formed by the immediately preceding region, V_{n-1}, and calculating the new radius, R_n:

$$R_n = \sqrt{\frac{V_{n-1} + \Delta V}{\pi}} \tag{5-3}$$

Azimuthal meshing is applied to the part by intersecting the cylindrical bodies that were formed by the RCC bodies with right angle wedge (RAW) bodies using the combinatorial geometry operation "RCC -RCC + RAW". The azimuthal mesh size is uniform in the part and is determined by calculating the delta angle, ΔA, from the input specifications provided by the user.

$$\Delta A = \frac{A_1 - A_0}{M} \tag{5-4}$$

where A_1 is the ending angle, A_0 is the starting angle, and M is the number of azimuthal meshes between the angles.

5.7 Volume and Material Identifiers

Parts and regions generated by the PMB code are identified using volume and material identifiers that are compatible with the RAMA model specifications. Volume identifiers are 32-character strings that allow parts and regions to be identified by a familiar name. Material identifiers are 32-character strings that describe the materials in the model.

The fully-qualified form of a volume identifier is:

PartName: PartNo.VolumeNo

where:

PartName	is a sub-string that identifies a part, or region, in the model;
":"	is a required field separator;
PartNo	is an integer value that identifies a specific instance of the part;
"."	is a required field separator; and
VolumeNo	is an integer value that identifies a sub-volume in the part.

Several parts with the same part name, *PartName*, may exist in a model. The different instances of the part are identified using part numbers, *PartNo*, starting with the integer value "1". A part may be composed of one or more sub-volume elements, *VolumeNo*, that are numbered starting with the integer value "1".

The fully-qualified form of a material identifier is:

MatName: MatNo

where:

MatName	is a sub-string that identifies a type of material;
":"	is a required field separator; and
MatNo	is an integer value that identifies a specific type of the material.

Several materials with the same material name, *MatName*, may exist in a model. The different instances of a material are identified using material numbers, *MatNo*, starting with the integer value "1".

6
MATERIAL PROCESSING METHOD

The purpose of the State-point Model Builder (SMB) code is to process reactor operating data and materials for assignment to the geometry model generated by the Parts Model Builder (PMB) code. The discrete materials and powers from the reactor operating data may be homogenized in the process. The material data handled by SMB includes nuclear fuel compositions for the reactor core region, steel compositions for structural components, and water compositions for the coolant flow regions.

The SMB provides the user with the capability to generate a homogenized bulk-core region and homogenized fuel elements that helps to reduce the model detail. Various types of fuel element homogenization are available. The homogenization methodology in SMB is based on volume weighted averaging of materials and powers. The subsections that follow describe the calculations performed in the State-point Model Builder code as a part of the homogenization process.

6.1 Fuel Assembly Homogenization

The reactor operating data from the utility generally contains considerable detail for the core region. Powers factors are provided for every fuel pin in every assembly, and compositions are provided for every fuel pin, water pin, channel and coolant bypass region in every assembly. These data may be homogenized into a single assembly, an assembly with fewer regions, or a bulk region. Full detail maybe preserved if desired.

The final result of the homogenization is determined by the geometry information in the PMB model files and, possibly, a PMB core region bulk homogenization file. The SMB code converts the reactor operating data into a form that matches the PMB geometry.

6.2 Volume Weighted Averaging

All homogenization is done using volume weighted averaging. Volume weighted averaging can be described by the equation:

$$\alpha = \frac{1}{V}\sum_{i=1}^{N} V_i \alpha_i \tag{6-1}$$

where V_i is the sub-volume, α_i is a property of that sub-volume, V is the total volume, and α is the homogenized property. The total volume is simply the sum of the sub-volumes:

$$V = \sum_{i=1}^{N} V_i \tag{6-2}$$

For example, to calculate the number density of a nuclide contained in the homogenized material, the product of the number density and volume for each composite region is summed over all regions and divided by the total volume. This is done for all the nuclides that are present.

6.2.1 Homogenization of the Relative Powers

The homogenization of the relative powers is handled somewhat differently than the other material properties. The approach is to conserve the power produced in the power producing regions in the homogenized region. RAMA generates the local region power density by taking the product of the global power density term and the local relative power factor. Thus the local region power density is determined by:

$$(pd)_i = r_i(PD) \tag{6-3}$$

where $(pd)_i$ is the power density in the i-th local region being modeled, r_i is the local relative power factor (field 3 in the RAMA GAT input block) for the i-th local region, and (PD) is the core average power density. Usually the global power density (PD) is specified as the average core power density for the plant, although this is a convention rather than a requirement. The only true requirement is that the product of the global power density and the local relative power factor in any region should produce the correct power density in that region.

The local power density of the i-th region in a RAMA model is defined as:

$$(pd)_i \equiv \frac{P_i}{V_i} \tag{6-4}$$

where P_i is the total power being produced in the i-th local region and V_i is the volume of the i-th local region as it is modeled in RAMA. The corresponding local relative power factor is obtained from Eqs. (6-3) and (6-4) as:

$$r_i = \frac{P_i}{V_i(PD)} \tag{6-5}$$

A check to confirm that the local relative power factors are consistent is to note that:

$$(PD)\sum_{i=1}^{N} r_i V_i = P_{TOT} \tag{6-6}$$

where N is the total number of modeled power producing regions in the core and P_{TOT} is the total power in the core (or total power in the modeled region of the core if the model is a subset of the full core).

The pin powers reported by the utilities are, invariably, the product of a nodal assembly relative power and a pin relative power, where the pin powers are normalized such that the average pin power taken over all pins results in the nodal power factor. The nodal power factor is the total nodal power divided by the power in an "average" core node. (Note that there is no dependence on volume in any of the utility reported power factors, other than the fact that the pin relative power factors are summed exclusively over the fuel pins, not all pincell regions in the node.)

This method of computing a relative pin power is somewhat inconsistent with the RAMA relative power term. This inconsistency shows up when the power in a given pin is computed using the utility definition of relative pin power versus the RAMA relative pin power definition. From the utility pin power definition, the total power in any pin node is given by:

$$P_i = p_i\left(\frac{P_{node}}{N_{pins}}\right) = p_i\left(\frac{P_{core}}{N_{nodes}N_{pins}}\right) \tag{6-7}$$

where p_i is the utility-specified relative pin power, P_{node} is the power in an average core node, P_{core} is the core power, N_{pins} is the number of fuel pins in the core node, and N_{nodes} is the number of nodes in the core (since all power nodes represented in the nodal codes have the same size).

The nodal pin total power computed by the RAMA definition is:

$$P_i = r_i V_i (PD) = r_i V_i\left(\frac{P_{core}}{V_{core}}\right) \tag{6-8}$$

where r_i is the RAMA relative pin power, V_i is the modeled volume of the pin, and V_{core} is the total core volume which is usually defined in RAMA runs as the total homogenized core volume, such that

$$V_{core} = N_{nodes}V_{node} \tag{6-9}$$

with V_{node} being the homogenized volume of a fuel node. From Eqs. (6-7), (6-8), and (6-9), the RAMA relative nodal pin power can be expressed as a function of the utility-supplied relative power as:

$$r_i = p_i \left(\frac{V_{node}}{V_i N_{pins}} \right) \tag{6-10}$$

If Eq. (6-10) is applied at the pin-by-pin level and if all fuel region volumes are assumed to be of equal size, then the RAMA relative pin powers are related to the utility-supplied relative pin powers by the following relationship:

$$r_i = p_i \left(\frac{V_{node}}{V_{fuel}} \right) \tag{6-11}$$

where V_{fuel} is the volume of fuel (i.e., power producing regions) in the modeled core node. It is important to note that Eq. (6-11) is applicable regardless of how the fuel pin volumes are considered in a model (i.e., the pins may be considered as discrete fuel rods, pincells within a channel, or even homogenized pincells over the entire core node). The only important thing is that, at the pin level, each fuel region can be represented with equal volumes.

Subsequent core node homogenization can now be accomplished using the "adjusted" RAMA pin powers from Eq. (6-11) as a starting point. The power in homogenized fuel regions should be determined using a volume weighted average of the individual regions that make up the homogenized region (including non-power producing regions). For example, a homogenized region consisting of N "pin" regions (some of which may have zero powers) would have a homogenized power of:

$$r_h = \frac{\sum_{i=1}^{N} r_i V_i}{\sum_{i=1}^{N} V_i} \tag{6-12}$$

where r_i is zero for non-power producing regions and the other individual region relative powers in Eq. (6-12) are related to the utility-supplied relative pin powers using Eq. (6-11). It should be noted that Eq. (6-12) can also be applied to situations involving homogenization of regions that lie on a diagonal symmetry line, which is commonly encountered in octant core models. The volume of those regions that are split by the symmetry line will have half the volume of the regions that are not split by the symmetry line.

As a simple example of the use of Eqs. (6-11) and (6-12), consider the case of an 8x8 fuel assembly node that has a nodal power factor of 0.3 with 62 fuel pins each having a relative

power (normalized to the nodal average) of 1.0 and two water rods. The utility-supplied relative pin powers for this node would be 0.3 for all power-producing fuel pins in the assembly node. Assuming the RAMA model consists of fuel pincells that are homogenized over the entire nodal volume (i.e., the channel and water gaps are not modeled as separate regions), then the ratio of the node volume to the fuel volume in Eq. (6-11) is given by:

$$\left(\frac{V_{node}}{V_{fuel}}\right) = \left(\frac{64 * V_{pincell}}{62 * V_{pincell}}\right) = 1.0323 \qquad (6\text{-}13)$$

The equivalent RAMA relative pin powers for a pin-by-pin representation of this assembly are 0.30968 [=0.3 * 1.0323] for each of the power-producing fuel regions.

Now consider the case of homogenizing the assembly node into quadrants composed of 4x4 fuel regions. Two of the quadrants will consist of 16 fuel rods and the other two quadrants will consist of 15 fuel rods and one water rod. The corresponding RAMA relative powers for the homogenized regions, from Eq. (6-12), are 0.30968 [=0.30968*16/16] in the quadrants containing 16 fuel rods and 0.29032 [= (15*0.30968+1*0.0)/16] in the quadrants containing 15 fuel rods and 1 water rod. Note that even this homogenization can be further homogenized to a single core node that has a RAMA relative power of 0.3000 [= (2*0.30968+2*0.29032)/4] or equivalently, [=(62*0.30968+2*0.0)/64]. If the entire assembly node is homogenized to a single region, then the RAMA relative power is equal to the assembly nodal relative power, as expected, regardless of how the homogenization is performed.

6.2.2 Homogenization of the Channel and Bypass Regions

In the case where the fuel assembly is homogenized into a single region or part of the bulk-core region, the materials of the channel and bypass are homogenized into the aggregate material using volume weighted averaging as outlined above. In the case where the fuel assembly (target geometry) has sub-regions or some form of pin detail and no channel or bypass detail, the materials of the channel and bypass must be distributed among the sub-regions according to the volume of the sub-regions. If the sub-regions are of equal volume, such as in full pin detail, the materials of the channel and bypass can be distributed evenly among the sub-regions, otherwise the relative volumes of the sub-regions must be considered.

6.3 Fuel Assembly RPP Types

Fuel assembly parts are described using Right Parallelepiped (RPP) bodies. A fuel assembly may be described as a single RPP region, as a set of RPP regions describing full pin detail, or as a special RPP type. Special RPP types allow partial assembly detail to be used. Some of the more commonly utilized RPP types are shown in Figure 6-1 and are identified as types 0, 1, 20, 26 and 28.

RPP type 0 has no sub-assembly detail, type 1 has full pin detail, and types 20, 26 and 28 have some form of homogenized detail. The actual size of the sub-regions in types 20, 26 and 28 depends on the geometry of the incoming data (i.e., the source or utility geometry).

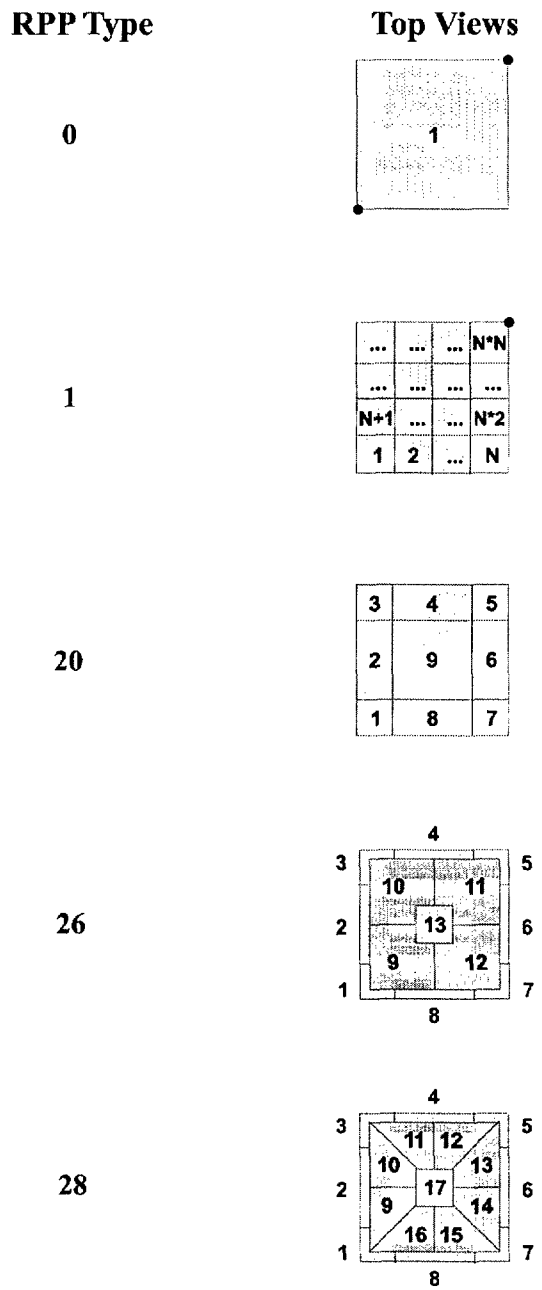

Figure 6-1
Rectangular Parallelepiped (RPP) Types

7
ACTIVATION, FLUENCE, AND UNCERTAINTY METHODS

The RAFTER code module of the RAMA Fluence Methodology calculates activation, fluence, and uncertainties for reactor components and regions in the reactor system. The methods used by RAFTER to perform these calculations and to determine nuclide activation and neutron fluence are presented in this section.

7.1 Activation Evaluation

Activation of material in surveillance capsules or other regions of the reactor system results from neutron absorption by a target nuclide to form a product nuclide that is radioactive. The activity resulting from the combined production and decay of the product nuclide provides a measure of the neutron fluence accumulated during the irradiation period. It is possible to predict the level of activation of the sample provided an estimate of the neutron flux is available.

7.1.1 Nuclide Activation

The differential equation that describes the rate of change in the number density of the target nuclide is given by:

$$\frac{dN_t}{dt} = -\sigma_a^t \phi N_t \tag{7-1}$$

where N_t is the number density of the target nuclide, σ_a^t is the absorption cross section for the target nuclide, and ϕ is the neutron flux. Note that the absorption is actually a function of energy, given by the expression:

$$\sigma_a^t \phi \equiv \sum_{g=1}^{\#groups} \sigma_{a_g}^t \phi_g \tag{7-2}$$

where $\sigma_{a_g}^t$ is the energy group-dependent absorption cross section of the target nuclide, and ϕ_g the group dependent neutron flux (that is assumed to be constant over the time interval of interest). Letting N_{t_0} be the target nuclide number density at time $t=t_0$, and assuming that the neutron flux is constant over the time interval $t > t_0$, then the target nuclide number density at time t ($t > t_0$) is determined from integration of Eq. (7-1) to be:

$$N_t(t) = N_{t_0} e^{-\sigma_a^t \phi (t-t_0)} \tag{7-3}$$

The differential equation that describes the rate of change in the number density of the product nuclide can be expressed in terms of production and loss of product nuclides as:

$$\frac{dN_p}{dt} = \sigma_R \phi N_t - (\lambda_p + \sigma_a^p \phi) N_p \tag{7-4}$$

where N_p is the number density of the product nuclide, λ_p is the product nuclide decay constant, σ_a^p is the absorption cross section of the product nuclide, and σ_R is the reaction response cross section (i.e., the cross section for product production from target irradiation). Note that the reaction response cross section for product production from fissions is equal to the target nuclide fission cross section multiplied by the product nuclide fission yield. Both the product absorption term and the reaction response term are also energy group dependent and are given by expressions similar to Eq. (7-2) by substituting the appropriate group-dependent cross section for the target absorption cross section in Eq. (7-2).

Substituting Eq. (7-3) into Eq. (7-4) yields:

$$\frac{dN_p}{dt} + (\lambda_p + \sigma_a^p \phi) N_p = \sigma_R \phi N_{t_0} e^{-\sigma_a^t \phi (t-t_0)} \tag{7-5}$$

Eq. (7-5) can be solved to yield:

$$N_p(t) = \left(N_{p_0} - \frac{\sigma_R \phi N_{t_0}}{\lambda_p + \sigma_a^p \phi - \sigma_a^t \phi} \right) e^{-(\lambda_p + \sigma_a^p \phi)(t-t_0)} + \left(\frac{\sigma_R \phi N_{t_0}}{\lambda_p + \sigma_a^p \phi - \sigma_a^t \phi} \right) e^{-\sigma_a^t \phi (t-t_0)} \tag{7-6}$$

where N_{p_0} is the product number density at time $t=t_0$. It should be noted that the product absorption rate is generally negligible while the target absorption rate is often negligible except for certain thermal reactions (such as ^{10}B absorption).

The activity resulting from the decay of the product nuclide is then given by:

$$A(t) = \lambda_p N_p(t) \tag{7-7}$$

for time $t \geq t_0$.

7.1.2 Accumulated Activation

The measured activity of dosimetry samples is the result of irradiation of the samples at varying flux magnitudes and energy distributions over a defined irradiation period. Variations in flux spatial and energy distributions result from reactor power variations and fuel exposure

accumulation. Reactor power and exposure effects must be accounted for in order to accurately estimate the activity of dosimetry samples at the end of the irradiation period.

One method of dealing with these operating history effects is to assume that the reactor power history can be treated as a series of step changes in power over time. The magnitude of the flux at these different power levels is assumed to be directly proportional to the reactor power. Since exposure effects are accumulated rather slowly throughout the irradiation period, it is also reasonable to assume that the energy distributions of the flux are relatively constant over several adjacent power steps.

Figure 7-1 shows an example of reactor power history over a period of time ranging from T_0 to T_{11}. In this example, the operating history is composed of ten discrete power levels that span three "state points". Each state point represents a period of time wherein the flux space and energy distributions are assumed to be constant.

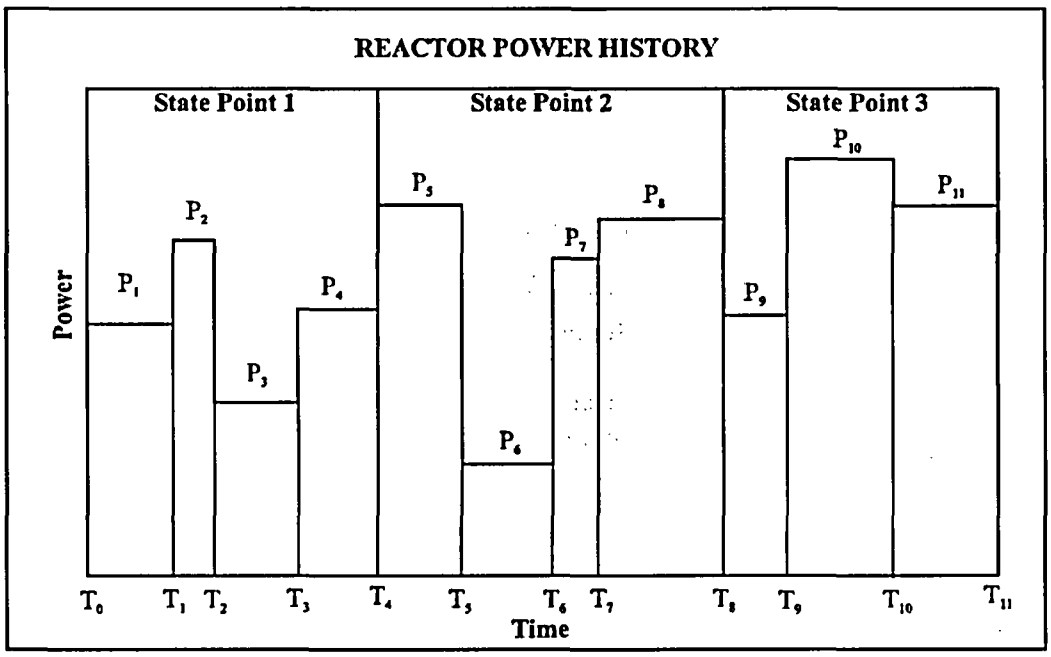

Figure 7-1
Reactor Operating History Example

In theory, large changes in reactor power would be expected to have an impact on the space and energy distributions of the flux, (e.g., due to variations in number densities) even if the changes occurred over small time periods. As a result, adjacent power steps with significantly different power levels would be expected to be represented by somewhat different state points. In practice, however, the selection of state points is often restricted to selected times with documented reactor operating conditions (such as process computer edit times). In addition, the irradiation of dosimetry located at the RPV or beyond is influenced less by the core interior bundles (that would be expected to be significantly more affected by the power changes) than by the core periphery bundles.

The estimation of accumulated activity in surveillance samples is accomplished by direct application of Eqs. (7-3), (7-6) and (7-7) to each time step in the history. The target and product number densities at the end of each time step are the corresponding initial number densities for the subsequent time step. A particle transport evaluation is performed for each state-point condition to obtain the reference state-point flux for each state-point condition. The flux in each power step is the corresponding state-point flux scaled by the ratio of the time step reactor power to the state-point reactor power, i.e.:

$$\phi_i = \phi_{i,s} p_i \left(\frac{P_R}{P_s} \right) \tag{7-8}$$

where ϕ_i is the flux at the surveillance sample location during the i-th power step, ϕ_s is the reference flux at the surveillance capsule location from the s-th state point particle transport evaluation that applies to the i-th time step, P_R is the rated reactor power, P_s is the reactor power used for the s-th state point particle transport evaluation, and p_i is the reactor fractional power during the i-th time step given by:

$$p_i = \frac{P_i}{P_R} \tag{7-9}$$

where P_i is the reactor power during the i-th time step. Since the reference state point flux is assumed to be directly proportional to the reactor power, it is common to use the reactor rated power in the reference state point particle transport evaluation, even if the actual reactor power at the state-point time is not the rated power. In this way, the power ratio in Eq. (7-8) is unity.

Utilizing the approach of representing the reactor power history as a set of constant power time steps allows the target and product nuclide number densities at the end of the i-th time step to be expressed as:

$$N_{t_i} = N_{t_{i-1}} e^{-\sigma_a^t \phi_i \Delta T_i} \tag{7-10}$$

and

$$N_{p_i} = \left(N_{p_{i-1}} - \frac{\sigma_R \phi_i N_{t_{i-1}}}{\lambda_p + \sigma_a^p \phi_i - \sigma_a^t \phi_i} \right) e^{-(\lambda_p + \sigma_a^p \phi_i)\Delta T_i} + \left(\frac{\sigma_R \phi_i N_{t_{i-1}}}{\lambda_p + \sigma_a^p \phi_i - \sigma_a^t \phi_i} \right) e^{-\sigma_a^t \phi_i \Delta T_i} \tag{7-11}$$

The accumulated activity in the dosimeter region is then given by:

$$A = \lambda_p N_{p_T} \tag{7-12}$$

where N_{p_T} is the product nuclide number density at the end of irradiation.

7.1.3 Activation Reaction Rates

Various neutron fluence experiments report the measured activation of the dosimetry in terms of the activation reaction rates of the irradiated material in the dosimeter. The reaction rate (reactions/sec per cm^3) is given by:

$$R = \frac{1}{T}\int_0^T N_t(t)\sigma_R\phi(t)dt \tag{7-13}$$

or, utilizing the concept of the reactor power history, as:

$$R = \frac{1}{T}\sum_{i=1}^{\#timesteps} \sigma_R\phi_i \int_{T_{i-1}}^{T_i} N_t(t)dt \tag{7-14}$$

where T is the total irradiation time (seconds) determined by summing the individual time step durations. Substituting Eq. (7-3) into Eq. (7-14) and performing the indicated integration over each time step yields:

$$R = \frac{1}{T}\sum_{i=1}^{\#timesteps} \frac{\sigma_R\phi_i N_{t_{i-1}}(1 - e^{-\sigma_a^t\phi_i\Delta T_i})}{\sigma_a^t\phi_i} \tag{7-15}$$

where ΔT_i is the duration of the i-th time step.

Note that it would appear that the flux in the numerator and denominator of Eq. (7-15) would cancel, however, that is not the case since the product of the cross section and the flux actually represents a summation of the energy group dependent values over all energy groups as noted in Eq. (7-2).

In the case of numerical benchmarks, it is common practice to use a single state point with no operating power history to determine the predicted activation reaction rates in dosimeter regions of the problem. When this is the case, the activation reaction rate takes the form:

$$R = \sigma_R\phi_s N_{t_0} \tag{7-16}$$

7.1.4 Reactions Per Atom

The total number of reactions per target atom may be used either as an alternate means of determining irradiation damage, such as displacements per atom (dpa), or for determining the accumulation of product nuclides, such as helium accumulation resulting from irradiation of boron impurities in steel. The total reactions per atom over the period of irradiation is given by:

$$R_A = \sum_{i=1}^{\#timesteps} \sigma_R\phi_i\Delta T_i \tag{7-17}$$

7.1.5 Equivalent ^{235}U Fission Spectrum Flux and Cross Section

A common means of reporting benchmark activation rates is through the use of the "equivalent ^{235}U fission spectrum flux". This equivalent flux utilizes an equivalent ^{235}U fission spectrum dosimeter cross section defined as:

$$\sigma_{eq} = \sum_{g=1}^{\#energygroups} \sigma_{R_g} \chi_g \tag{7-18}$$

where χ_g is the energy group dependent ^{235}U fission production spectrum. The equivalent ^{235}U fission spectrum flux is then defined as:

$$\phi_{eq} = \frac{\sum_{g=1}^{\#energygroups} \sigma_{R_g} \phi_g}{\sigma_{eq}} \tag{7-19}$$

7.1.6 Response Function Nuclide Number Densities and Decay Constants

In order to facilitate the computation of activation reactions in support of RPV fluence and surveillance capsule evaluations, the RAFTER computer program includes default values of target nuclide number densities and product nuclide decay constants for the BUGLE-96 [2] response reactions. The target number densities given in Table 7-1 are based upon the natural abundance of the target nuclide. Table 7-2 contains the corresponding product decay constants for the various response reactions.

7.2 Neutron Flux and Fluence Evaluations

Determining the neutron fluence in component regions of reactor systems is an essential element in the assessment of component damage resulting from neutron irradiation. Generally, the evaluation is restricted to a reduced energy range since low energy neutrons are substantially less likely to inflict irradiation damage than are high-energy neutrons. Material damage assessments are usually restricted to neutron energies > 0.1 MeV, with neutron energies > 1 MeV being even more commonly used to express the extent of irradiation damage.

7.2.1 Neutron Flux Energy Cutoff

Since most reactor system component damage assessments are based upon flux values that are greater than a cutoff energy level, it is necessary to be able to compute flux values that do not span the entire energy spectrum used in the particle transport calculation. If the energy cutoff value falls on a group boundary, the resulting flux that is greater than the energy cutoff value is simply the sum of the fluxes in the energy groups with lower energy range values that are above the cutoff value. In this case, the resulting neutron flux is given by:

$$\phi_{i,E_0} = \sum_{g \leq G} \phi_{i,g} \tag{7-20}$$

where ϕ_{i,E_0} is the flux in the i-th state point with energy greater than the cutoff energy, E_0, G is the energy group whose lower boundary value coincides with the cutoff energy value, g is the group index, and $\phi_{i,g}$ is the neutron flux in energy group g for the i-th state point.

If the cutoff energy value does not coincide with a group boundary, then it is necessary to determine the contribution to the neutron flux from the energy group in which the cutoff energy value lies. In this case, the resulting neutron flux can be expressed as:

$$\phi_{i,E_0} = \sum_{g < G} \phi_g + \delta_G \tag{7-21}$$

where G is the energy group that the cutoff energy lies in and δ_G is the contribution from energy group G to the neutron flux that is greater than the cutoff energy. This contribution is determined in the same manner as described in Section 4.2.3.

Table 7-1
Default Target Nuclide Number Densities

Target Nuclide	Number Density (atoms/b-cm)
^{27}Al	6.0242E-02
^{197}Au	5.9074E-02
^{10}B	2.6276E-02
^{59}Co	9.0951E-02
^{63}Cu	5.8738E-02
^{65}Cu	2.6180E-02
^{54}Fe	4.9249E-03
^{56}Fe	7.7882E-02
^{58}Fe	2.3776E-04
^{127}I	2.3396E-02
^{115}In	3.6694E-02
^{6}Li	3.4750E-03
^{55}Mn	8.1451E-02
^{23}Na	2.5437E-02
^{58}Ni	6.2166E-02
^{60}Ni	2.3946E-02
^{237}Np	5.1448E-02
^{239}Pu	4.9967E-02
^{240}Pu	[1]
^{241}Pu	[1]
^{242}Pu	[1]
^{103}Rh	7.2629E-02
^{32}S	3.6949E-02
^{45}Sc	4.0042E-02
^{232}Th	3.0419E-02
^{46}Ti	4.5666E-03
^{47}Ti	4.1670E-03
^{48}Ti	4.2126E-02
^{234}U	2.5891E-06
^{235}U	3.4090E-04
^{236}U	[1]
^{238}U	4.7599E-02

[1] These nuclides do not have a naturally occurring nuclide number density.

Table 7-2
Default Product Nuclide Decay Constants

Product Nuclide	Decay Constant (1/sec)
^{198}Au	2.976E-06
^{58}Co	1.133E-07
^{60}Co	4.166E-09
^{64}Cu	1.516E-05
^{59}Fe	1.803E-07
^{4}He	Stable
^{126}I	6.118E-07
^{115m}In	4.292E-05
^{116m}In	2.128E-04
^{27}Mg	1.221E-03
^{54}Mn	2.569E-08
^{56}Mn	7.467E-05
^{24}Na	1.287E-05
^{57}Ni	5.407E-06
^{32}P	5.626E-07
^{103m}Rh	2.059E-04
^{46}Sc	9.575E-08
^{47}Sc	2.401E-06
^{48}Sc	4.409E-06
^{233}Th	5.180E-04
^{239}U	4.926E-04

7.2.2 Accumulated Neutron Fluence

The accumulated fluence greater than an energy cutoff value of E_0 in a region is given by:

$$\varphi_{E_0} = \sum_{i=1}^{\#timesteps} \phi_{i,E_0} \Delta T_i \tag{7-22}$$

where ΔT_i is the duration of the i-th time step in seconds and ϕ_{i,E_0} is the accumulated neutron flux above the energy cutoff value E_0 as determined from Eq. (7-20) or Eq. (7-21).

7.2.3 Effective Full Power Time

The effective full power time (seconds) is given by:

$$T_E = \sum_{i=1}^{\#timesteps} p_i \Delta T_i \tag{7-23}$$

where ΔT_i is the duration in seconds of the i-th time step and p_i is the fractional power factor given in Eq. (7-9).

7.2.4 Cumulative Power Factor

The cumulative power factor is the average fractional power of the reactor over the period of irradiation and is given by:

$$\overline{p} = \frac{\sum_{i=1}^{\#timesteps} p_i \Delta T_i}{T} = \frac{T_E}{T} \tag{7-24}$$

where T_E is the effective full power time given by Eq. (7-23) and T is the total time of irradiation given by the sum of the duration of all time steps in the irradiation period. This value is analogous to the plant capacity factor for the period.

7.2.5 Average Neutron Flux

When reactor power history is provided, the region average neutron flux for energy above an energy cutoff value of E_0 is given by:

$$\overline{\phi}_{E_0} = \frac{\sum_{i=1}^{\#timesteps} \phi_{i,E_0} \Delta T_i}{T} \tag{7-25}$$

where T is the total irradiation time given by the sum of the duration of all time steps in the irradiation period.

When no reactor power history is provided, the region average neutron flux for energy above an energy cutoff value of E_0 can be determined directly from the state-point flux value:

$$\overline{\phi}_{E_0} = \phi_{s,E_0} \tag{7-26}$$

where ϕ_{s,E_0} is the state-point flux above the energy cutoff value of E_0 computed using Eq. (7-20) or Eq. (7-21) as appropriate.

7.2.6 Rated Power Neutron Flux

The rated power neutron flux above an energy cutoff value of E_0 provides a means for estimating the end of life fluence of the reactor components. The rated power neutron flux is given by:

$$\phi_{R,E_0} = \frac{\sum_{i=1}^{\#timesteps} \phi_{i,E_0} \Delta T_i}{\sum_{i=1}^{\#timesteps} p_i \Delta T_i} = \frac{\sum_{i=1}^{\#timesteps} \phi_{i,E_0} \Delta T_i}{T_E} \tag{7-27}$$

where T_E is the effective full power time from Eq. (7-23).

7.3 Uncertainty Analysis Methodology

The neutron flux undergoes several decades of attenuation between the core and the reactor pressure vessel. Calculation of the neutron flux distribution is sensitive to material and geometric representation of the core and reactor internals, the neutron source, the nuclear cross-section data, and the numerical scheme used in the calculation. It is important to account for uncertainties in these parameters in determining the neutron fluence and in estimating the uncertainty in the calculated fluence.

The sources of uncertainty in determining the RPV fluence include analytical uncertainty and comparison uncertainty. These are combined to provide an estimate of the overall fluence bias and standard deviation that is used to determine the best-estimate RPV fluence from the calculated RPV fluence values. The methods used to calculate these forms of uncertainty are presented in the following subsections.

7.3.1 Analytical Uncertainty

The uncertainty analysis applied to the neutron fluence calculation is a function of several random, possibly correlated, input parameters. The calculated neutron fluence (>1 MeV) at any given location in the RPV can be expressed in functional form as:

$$\phi = \phi(x_1, x_2, \ldots, x_n) = \phi(\bar{x}) \tag{7-28}$$

where ϕ is the resultant neutron fluence that is a function of the N input parameters: x_1, x_2, ... x_n (represented by the N-dimensional vector $\bar{x}$). Using a linear approximation (single term Taylor expansion), the fluence corresponding to a perturbed set of input parameters can be written as:

$$\phi(\bar{x} + \delta\bar{x}) = \phi(\bar{x}) + \delta\phi = \phi(\bar{x}) + \sum_{i=1}^{n} \frac{\partial\phi}{\partial x_i}\delta x_i \tag{7-29}$$

From Eq. (7-29), the deviation in fluence resulting from deviations in the input parameters can be written in matrix form as:

$$\delta\phi = S_a^T(\delta\bar{x}) \tag{7-30}$$

where S_a is the N-dimensional sensitivity vector corresponding to deviations in the analytical input parameters, $\delta\bar{x}$ is the N-dimensional vector of deviations in input parameter values, and the superscript T denotes the transpose of the vector. The sensitivity vector takes the general form of:

$$S_a = \begin{bmatrix} \frac{\partial\phi}{\partial x_1} \\ \cdots \\ \frac{\partial\phi}{\partial x_n} \end{bmatrix} \approx \begin{bmatrix} \frac{\Delta\phi}{\Delta x_1} \\ \cdots \\ \frac{\Delta\phi}{\Delta x_n} \end{bmatrix} \tag{7-31}$$

The statistical standard deviation corresponding to the analytical fluence evaluation can be determined from Eq. (7-30) to be:

$$\sigma_a \equiv \left[E\left\{(\delta\phi)(\delta\phi)^T\right\}\right]^{1/2} = \left[S_a^T E\left\{(\delta\bar{x})(\delta\bar{x})^T\right\}S_a\right]^{1/2} = \left[S_a^T C_a S_a\right]^{1/2} \tag{7-32}$$

where the notation E{ } denotes the statistical expectation (i.e., an average over a probability distribution of possible deviations from the mean value) and C_a is the N x N uncertainty matrix (i.e., covariance matrix) that describes the uncertainty of the input parameters. The uncertainty matrix in Eq. (7-32) takes the form:

$$C_a = \begin{bmatrix} \sigma_1^2 & \sigma_{12}^2 & \cdots & \sigma_{1N}^2 \\ \sigma_{21}^2 & \sigma_2^2 & \cdots & \sigma_{2N}^2 \\ \cdots & \cdots & \cdots & \cdots \\ \sigma_{N1}^2 & \sigma_{N2}^2 & \cdots & \sigma_N^2 \end{bmatrix} \tag{7-33}$$

The diagonal elements of the uncertainty matrix are the statistical variances (i.e., squares of the standard deviations) of the corresponding input parameters. The off-diagonal elements are statistical covariances that describe the correlation between the input parameters, if any correlation exists. It should be noted that most of the input parameters that comprise the analytical uncertainty evaluation are uncorrelated, therefore, the corresponding off-diagonal elements of the uncertainty matrix are zero.

The fluence calculation methodology may result in an inherent analytical bias in the determination of the RPV fluence. It is possible to estimate the relative analytical bias from Eq. (7-30) as:

$$B_a = \frac{\phi(\bar{x}_{opt}) - \phi(\bar{x}_a)}{\phi(\bar{x}_a)} \approx \frac{S_a^T(\bar{x}_{opt} - \bar{x}_a)}{\phi(\bar{x}_a)} \tag{7-34}$$

where $\bar{x}_a$ is the vector of input parameters used in the analytical fluence evaluation and $\bar{x}_{opt}$ is the vector of "optimal" input parameters that, when used in the fluence evaluation, produce the best estimate of the fluence. The components of the "optimal" input parameter set consist of the mean value of input parameters that are bounded (such as parameters with tolerances or estimate uncertainty ranges) and the asymptotic value of input parameters that are unbounded (such as mesh interval parameters and angular quadrature set parameters). In general, the mean value of bounded input parameters is used in the standard fluence evaluation, so the contribution to the analytical fluence bias is zero for these parameters. However, it is not uncommon that values other than the true asymptotic value of unbounded input parameters are used in the standard fluence evaluation. This can result in a non-zero analytical bias.

The analytical input parameter set and the corresponding uncertainty in the input parameters is expected to be somewhat application specific. An example of a "typical" input parameter set that would be applicable to fluence evaluations in BWRs is shown in Table 7-3. The type of analysis used to obtain the sensitivity elements that comprise the sensitivity vector is also shown in Table 7-3. The spectral effects resulting from the flux attenuation through the RPV is accounted for in the analytical uncertainty analysis by computing individual bias and standard deviation values at the 0 T, ¼ T, ½ T, ¾ T, and T locations at the azimuth of peak vessel fluence (for 2-D sensitivity cases) and at the azimuth and axial location of peak vessel fluence (for 3-D sensitivity cases).

Table 7-3
Sample Input Parameter Set

Content Deleted -
EPRI Proprietary Information

7.3.2 Comparison Uncertainty

The comparison uncertainty is determined from the comparison between measured and calculated dosimetry activation results obtained from the fluence benchmark and operating reactor surveillance capsule evaluations. Uncertainties in the comparison to measured values arise from (1) uncertainties in the predicted activities due to uncertainties in calculation input parameters, and (2) uncertainties in the measured activities. The comparison uncertainty analysis accounts for both of these contributions.

The calculated flux is used to determine calculated activities at the dosimeter locations. Uncertainties in the calculated activities are determined in a similar manner to the calculated vessel fluence uncertainties described in Section 7.3.1. Sensitivity evaluations are performed for each measurement in the benchmark and operating plant surveillance capsule database.

For a measurement database consisting of M measurements and a set of N significant input parameters used in the activation calculation, then the N x M sensitivity matrix obtained from sensitivity evaluations is given by:

$$S_I = \begin{bmatrix} \frac{\partial A_1}{\partial x_1} & \frac{\partial A_2}{\partial x_1} & \cdots & \frac{\partial A_M}{\partial x_1} \\ \frac{\partial A_1}{\partial x_2} & \frac{\partial A_2}{\partial x_2} & \cdots & \frac{\partial A_M}{\partial x_2} \\ \cdots & \cdots & \cdots & \cdots \\ \frac{\partial A_1}{\partial x_N} & \frac{\partial A_2}{\partial x_N} & \cdots & \frac{\partial A_M}{\partial x_N} \end{bmatrix} \approx \begin{bmatrix} \frac{\Delta A_1}{\Delta x_1} & \frac{\Delta A_2}{\Delta x_1} & \cdots & \frac{\Delta A_M}{\Delta x_1} \\ \frac{\Delta A_1}{\Delta x_2} & \frac{\Delta A_2}{\Delta x_2} & \cdots & \frac{\Delta A_M}{\Delta x_2} \\ \cdots & \cdots & \cdots & \cdots \\ \frac{\Delta A_1}{\Delta x_N} & \frac{\Delta A_2}{\Delta x_N} & \cdots & \frac{\Delta A_M}{\Delta x_N} \end{bmatrix} \tag{7-35}$$

where A_m is the predicted relative activity corresponding to the m-th measurement in the database, and x_n is the n-th significant input parameter in the sensitivity evaluation. The list of input parameters that are included in the comparison uncertainty sensitivity evaluation are generally similar to those utilized in the fluence analytical uncertainty sensitivity evaluation with some additional activity calculation specific parameters, such as detector location and activation cross sections.

Letting C_x be the N x N uncertainty matrix associated with the input parameters and C_m be the M x M uncertainty matrix associated with the measurements, then the uncertainty associated with the difference between calculated and measured results, C_d, is given by:

$$C_d = S_I^T C_x S_I + C_m \tag{7-36}$$

where it has been assumed that there is no correlation between the input parameters and the measured results. For a detailed derivation of Eq. 7-36, see [8]. If $\bar{d}$ is the M-dimensional vector whose elements are the differences between the calculated and measured activity results, then the overall comparison uncertainty (i.e., standard deviation) can be expressed as:

$$\sigma_b = \left[\bar{d}^T C_d \bar{d}\right]^{1/2} \tag{7-37}$$

The bias, based upon comparison of calculated to measured dosimeter results, is:

$$B_b = \sum_{i=1}^{M} \frac{m_i - c_i}{c_i} = \sum_{i=1}^{M} \left(\frac{m_i}{c_i} - 1 \right) \tag{7-38}$$

where m_i is the i-th measured activation value in the database and c_i is the i-th calculated activation value. Note that an implicit assumption in Eq. (7-38) is that the relative bias based upon comparison to measured values applies to RPV locations as well.

The elements contributing to the comparison uncertainty analysis are generally quite different for the vessel simulator benchmark evaluations as opposed to operating light water reactor dosimetry evaluations. As a result, the bias and uncertainty (standard deviation) are determined using the above methodology for two different measurement databases: (1) the vessel simulator benchmark database consisting of comparison results for the PCA and VENUS-3 benchmark problems, and (2) the operating system database consisting of dosimetry measurement data from operating light water reactor plants.

The comparison databases must be evaluated to confirm their statistical validity for use in determining the RPV "best estimate" bias. Statistical valid databases must meet three criteria: (1) the database should provide a representative sample over the range of operating states for which the fluence evaluation methodology is to be applied, (2) the uncertainty in the database comparisons should be small compared to the comparison bias, and (3) the calculation and measurement errors of the comparison ratios must be uncorrelated (i.e., no systematic bias is present in the comparisons).

The method of evaluating the extent of correlated comparisons in the databases, and the method for removing the correlated bias is described in [9]. The database comparisons are expressed in a regression model of the form:

$$\left(\frac{m}{c} \right) = \mu_{m/c} + \sum_{k=1}^{K} c_k \alpha_k \tag{7-39}$$

where $\mu_{m/c}$ is the fitted mean of the comparisons, c_k are fit coefficients, and α_k are parameters that represent various possible correlation conditions, such as the type of detector, the location of the detector (e.g., in-vessel and behind jet pumps), the energy threshold of the detector, etc. The statistics of the fit parameters are used to determine correlated parameters. The regression model of Eq. (7-39) is used to remove the systematic bias from the measurement comparisons. The measurement comparisons are used to determine an adjusted bias, as in Eq. (7-38).

7.3.3 Combined Uncertainty

Content Deleted -
EPRI Proprietary Information

(7-40)

(7-41)

Content Deleted -
EPRI Proprietary Information

(7-42)

(7-43)

7.3.4 Best Estimate Fluence

The combined fluence bias and standard deviation determined from Section 7.3.3 are used to compute the best estimate neutron fluence from the calculated fluence as specified in [1] using the following methodology.

If the combined standard deviation is ≤20%, the best estimate neutron fluence is

$$\varphi = \varphi_c(1 + B_c) \tag{7-44}$$

where φ_c is the calculated neutron fluence and B_c is the combined fluence bias. If the combined standard deviation is greater than 20% but less than 30%, the best estimate neutron fluence is

$$\varphi = \varphi_c\left(1 + B_c + \frac{\sigma_c(\%) - 20}{100}\right) \tag{7-45}$$

where σ_c is the combined fluence standard deviation from Eq. (7-43).

[This page intentionally left blank]

8
NUCLEAR DATA GENERATION METHOD

The RAMA nuclear data library is derived from the BUGLE-96 [2] nuclear data library. BUGLE-96 is comprised of several data files containing material cross sections, response functions, and kerma factors that are appropriate for LWR shielding and pressure vessel dosimetry calculations. RAMA is a single data library file that contains the necessary data from the various BUGLE-96 data files. The following subsections describe the process for generating the RAMA nuclear data library.

8.1 BUGLE-96 Data

The BUGLE-96 and RAMA cross section data is represented in a coupled 47 neutron/20 gamma-ray broad-group, energy group structure with scattering cross section moments up to P_7. The 47 neutron/20 gamma-ray broad-group cross sections were derived from the fine-group VITAMIN-B6 [10] nuclear data library using the SCAMPI [11] code package. The BUGLE-96 library includes several sets of weighted broad-group data that are weighted according to location and flux spectra in the reactor. This means that the data that will be used in transport calculations has been collapsed from a fine-group to a broad-group structure using a flux spectrum that is appropriate for the region containing the material. As a consequence, several forms of the same material are included in the library, each weighted with a different flux spectrum. Collapsed data are included for the following reactor regions: BWR core, downcomer, pressure vessel, and concrete shield.

The broad-group cross section data, response functions, and kerma factors in the RAMA nuclear data library are derived directly from the BUGLE-96 nuclear data library. The cross section data is obtained from the self-shielded data with thermal up-scatter.

8.2 Nuclide Identifiers

The BUGLE-96 and RAMA nuclear data libraries use different identifiers to identify the materials and nuclides in the data libraries. BUGLE-96 uses "material numbers" and RAMA uses "nuclide identifiers". There is no direct correspondence of the BUGLE-96 material numbers with RAMA nuclide identifiers.

The material numbers used in the BUGLE-96 nuclear data library define one cross section set with one scattering moment for a nuclide. The material numbers are assigned in a somewhat arbitrary fashion; that is, the numbers do not necessarily identify a particular nuclide for the data. The only requirements for material numbers is that each material number in the data library must be unique in order to select the correct cross section set for a transport calculation.

The nuclide identifiers in the RAMA nuclear data library are specified to permit the data to be easily identified and associated with a particular nuclide. RAMA nuclide identifiers are specified by an integer value of the form "ZZAAAWW", where ZZ is the atomic number, AAA is the atomic weight, and WW is a spectrum weighting identifier. Whereas BUGLE-96 maintains separate material cross section tables for each Legendre scattering moment, RAMA maintains one nuclide identifier that represents all the scattering moments for that nuclide.

8.3 Legendre Order of Scattering

The cross section sets in the BUGLE-96 and RAMA nuclear data libraries include high-order scattering moments for treating anisotropic effects in the transport calculations. The order of scattering is based upon a Legendre expansion of the scattering term. The same order of scattering is used for both neutrons and gamma-rays. The highest moments in the RAMA and BUGLE-96 data libraries are P_7 for nuclides with Z=1 (hydrogen) to Z=29 (copper) and P_5 for the remainder of the nuclides.

RAMA is capable of performing anisotropic calculations using scattering moments from P_1 through P_7. The order of scattering may be specified by the user. Even though all cross sections are not tabulated with the same scattering moments (i.e., some nuclides have P_5 and some have P_7 tabulations), RAMA properly handles situations when higher order (greater than P_5) cross sections are mixed with lower order (less than or equal to P_5) cross sections.

8.4 Cross Section Generation

The BUGLE-96 nuclear data library includes nuclear cross section data that are specifically developed for light water reactor shielding and pressure vessel dosimetry calculations. These cross sections are generated from the VITAMIN-B6 nuclear data library using the SCAMPI code package. The process used to generate the light water reactor cross sections for both BWR and PWR reactors is described in the BUGLE-96 distribution documentation.

The RAMA nuclear data library contains cross section data for the same material nuclides as the BUGLE-96 nuclear data library. In addition, the RAMA data library includes BWR and PWR core-weighted cross section data for the following actinides: ^{239}Pu, ^{240}Pu, ^{241}Pu, and ^{242}Pu, as well as fission cross section data and fission spectrum data for ^{235}U, ^{238}U, ^{239}Pu, ^{240}Pu, ^{241}Pu, and ^{242}Pu. The additional BWR and PWR core-weighted actinide cross section data is generated from VITAMIN-B6 using the same basic process as that used to generate BUGLE-96. The methodology for generating the additional core-weighted RAMA cross sections from VITAMIN-B6 and for generating the composite RAMA nuclear data library involves four major steps:

1. Perform resonance shielding of the additional BWR and PWR actinide nuclides from the VITAMIN-B6 BCD data files using generic BWR or PWR pincell geometry and material composition, as appropriate.

2. Collapse the fine-group shielded working library cross sections to the desired broad-group structure (47 neutron / 20 gamma-ray) using the BUGLE-96 BWR or PWR core region collapsing flux spectra, as appropriate.

3. Create an ANISN BCD format library containing the broad-group cross sections.

4. Generate the RAMA binary nuclear data library using the BUGLE-96 light water reactor weighted cross-section data combined with the additional BWR and PWR core-weighted nuclear data generated in steps 1 through 3 above.

Figure 8-1 illustrates steps 1 through 3 that involves running the SCAMPI code modules to generate the additional BWR or PWR core-shielded cross sections in ANISN-format. The additional nuclear data is then combined with the remaining BUGLE-96 light water reactor data to form the RAMA nuclear data library. Figure 8-2 illustrates step 4 that involves running the RAMALIB code to generate the RAMA nuclear data library file.

The BUGLE-96 data library contains most of the nuclides required by the RAMA code system for light water reactor fluence calculations except plutonium and selected uranium nuclear data. Therefore, it is only necessary to run the SCAMPI code system to process additional uranium cross sections for the uranium nuclides ^{235}U and ^{238}U and the additional plutonium cross sections for the plutonium nuclides ^{239}Pu, ^{240}Pu, ^{241}Pu, and ^{242}Pu.

The four steps required to generate the RAMA nuclear data library file are described in more detail in subsections that follow.

8.4.1 Generation of Resonance Self-shielded Actinide Cross Sections

The SCAMPI code system is used to generate a working library that contains appropriately shielded corrections for common resonance nuclides.

Following is a description of the process involved in generating the resonance self-shielded cross sections for the BWR and PWR actinide nuclides:

1. The AIM and AJAX modules of SCAMPI are executed for each core nuclide to convert the VITAMIN-B6 BCD format data files into a binary unshielded master library.

2. Appropriately self-shielded core actinide cross sections are obtained by executing the BONAMI module of SCAMPI material and geometry definitions provided in [4] for BWR and PWR fuel pincells.

3. The AJAX module is again executed to produce a set of cross sections in AMPX binary master library format that contains the desired self-shielded actinide nuclides in the VITAMIN-B6 group structure (i.e., 199 neutron groups and 42 photon groups).

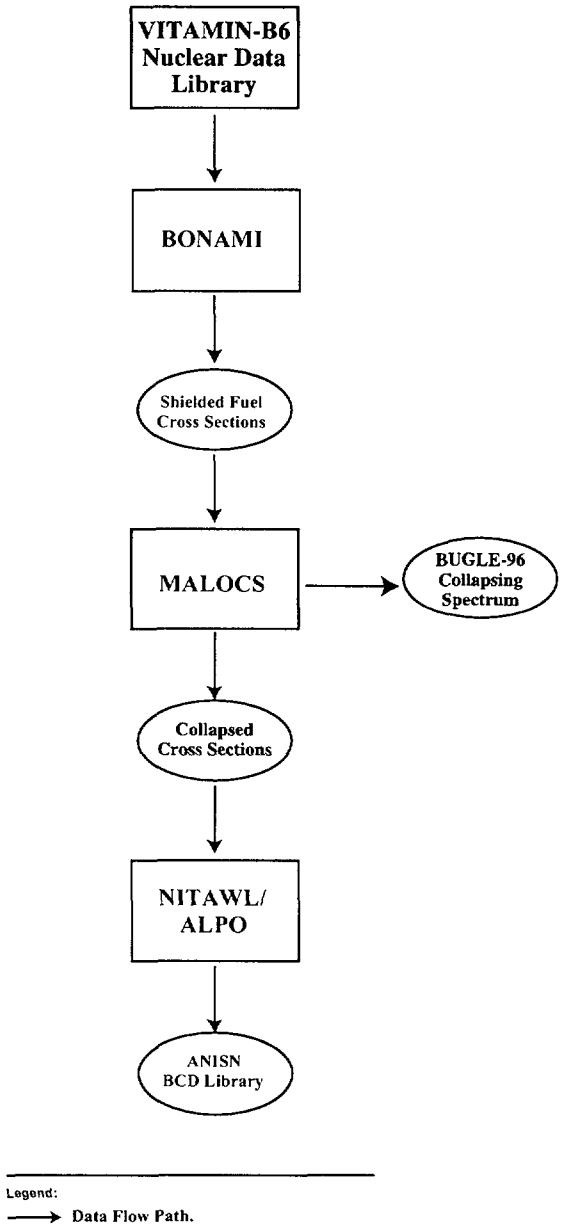

Figure 8-1
SCAMPI Cross Section Processing Flow Diagram

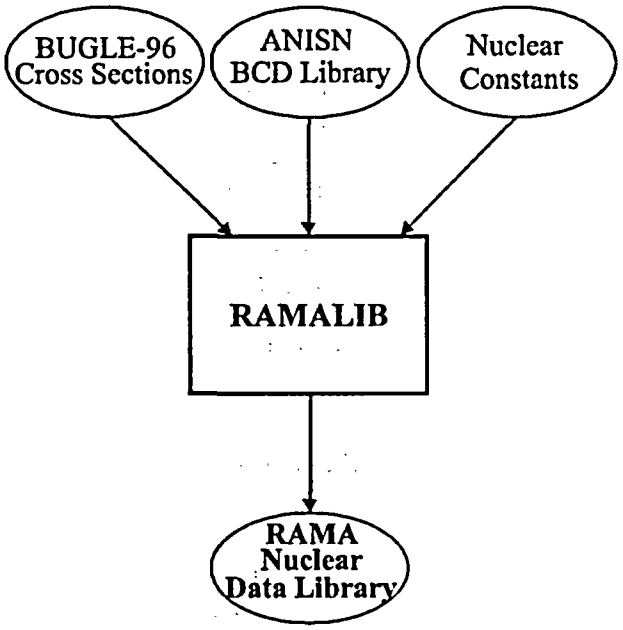

Legend:
——▶ Data flow path.

Figure 8-2
RAMA Nuclear Data Library Generation Flow Diagram

8.4.2 Generation of Broad Group Shielded Cross Sections

The self-shielded actinide cross sections obtained from step 1 are collapsed to the BUGLE-96 and RAMA broad-group structure (i.e., 47 neutron groups and 20 photon groups). The flux spectra used to collapse the cross sections are the same as those used to collapse the BUGLE-96 core-weighted nuclides. These spectra have been determined from generic 1-D BWR and PWR reactor system models using the XSDRNPM module of the SCAMPI package.

Following is a description of the process used to collapse the BWR and PWR self-shielded actinide cross sections obtained from the process described in Section 8.4.1 above to a set of BWR and PWR core-weighted nuclides in the AMPX working library format and BUGLE-96 energy group structure:

1. The MALOCS module of SCAMPI is executed to collapse the self-shielded actinide nuclide cross sections to the BUGLE-96 energy group structure. The collapsing process uses the appropriate collapsing flux spectra from [2] (i.e., the BWR flux distribution from region #57 of the XSDRNPM BWR reactor system model and the PWR flux distribution from region #37 of the XSDRNPM PWR reactor system model).

2. The collapsed core-weighted cross sections are converted to the AMPX working library format by the NITAWL module of SCAMPI.

3. The RADE module of SCAMPI is executed to perform consistency and validity checks on the collapsed set of cross sections to ensure that the data is free of obvious processing errors.

8.4.3 Creation of ANISN BCD Nuclear Data

The final RAMA library generation process requires that the nuclear data for all nuclides be in the ANISN BCD format (either fixed-format or free-format). The BUGLE-96 nuclear data is in ANISN BCD fixed format. The additionally processed actinide nuclear data must be converted to ANISN BCD format in order to be included in the RAMA nuclear data library.

Following is a description of the process used to convert the collapsed core-weighted BWR and PWR cross sections obtained from Section 8.4.2 above to ANISN BCD format libraries for incorporation in the RAMA nuclear data library generation process.

1. The conversion of the collapsed core-weighted cross sections to ANISN BCD format libraries is performed by the ALPO module of SCAMPI. In addition to the traditional cross section arrays that are typically provided with the BUGLE-96 nuclide data sets (i.e., absorption, nu-fission, total, and scattering matrix cross sections), additional data arrays (i.e., fission cross section and fission spectrum arrays) are included in the BWR and PWR actinide ANISN libraries. The resulting ANISN BCD libraries are assigned to named data files that are used along with the remaining BUGLE-96 nuclide data files to generate the RAMA nuclear data library as described in Section 8.4.4 of this manual.

2. To assist in verifying the validity of the created actinide ANISN libraries, the LAVA module of SCAMPI is used to convert the BCD libraries back into AMPX working library format cross-section sets.

3. The ALE module of SCAMPI is then used to display the nuclide data arrays (e.g., total cross section array, absorption cross section array, etc.). The data arrays for core-weighted ^{235}U and ^{238}U can then be compared to the corresponding data arrays obtained from the same BUGLE-96 nuclear data library.

8.4.4 Generation of the RAMA Nuclear Data Library

The RAMALIB code is used to generate the RAMA nuclear data library from the ANISN BCD cross section data files generated by the SCAMPI code system and other nuclear constants. RAMALIB uses one input file to describe all the data required for the RAMA nuclear data library. This input file includes references to the individual nuclide data files that contain the cross-section data for the nuclide. The file also provides for assigning kerma values, kappa values (i.e., energy release per fission), and the RAMA nuclide identifier to the individual nuclides.

[This page intentionally left blank]

9
REFERENCES

1. "Calculational and Dosimetry Methods for Determining Pressure Vessel Neutron Fluence," Nuclear Regulatory Commission Regulatory Guide 1.190, March 2001.

2. "BUGLE-96: Coupled 47 Neutron, 20 Gamma-Ray Group Cross Section Library Derived from ENDF/B-VI for LWR Shielding and Pressure Vessel Dosimetry Applications," RSICC Data Library Collection, DLC-185, March 1996.

3. "Programming Languages – Fortran," ISO/IEC, 1559-1:1997, International Organization for Standardization and International Electrotechnical Commission, October 21, 1997.

4. "C Programming Language," ANSI X3.159-1989, American National Standards Institute, Inc., December 14, 1989.

5. J. T. West, M. B. Emmett, "MARS: A Multiple Array System Using Combinatorial Geometry," Oak Ridge National Laboratory, Radiation Shielding Information Center report, December 1980.

6. H. Lichtenstein, et al, "The SAM-CE Monte Carlo System for Radiation Transport and Criticality Calculations in Complex Configurations," CCM-8, EPRI Research Project 972, 1980.

7. G. I. Bell and S. Glasstone, "Nuclear Reactor Theory," Van Nostrand Reinhold Company, 1970, p. 65.

8. B. L. Broadhead, C. M. Hopper, and C. V. Parks, "Sensitivity and Uncertainty Analyses Applied to Criticality Safety Validation," NUREG/CR-6655, Vol. 2, Nov. 1999.

9. J. Carew, S. Finch, and L. Lois, "Statistical Analysis of Reactor Pressure Vessel Fluence Calculation Benchmark Data Using Multiple Regression Techniques," *Nuclear Science and Engineering*, 143, 2003, pp. 158-163.

10. "VITAMIN-B6: A Fine-Group Cross Section Library Based on ENDF/B-VI Release 3 for Radiation Transport Applications," RSICC Data Library Collection, DLC-184, December 1996.

11. "SCAMPI: Collection of Codes for Manipulating Multigroup Cross Section Libraries in AMPX Format," RSICC Computer Code Collection, PSR-352, September 1995.

[This page intentionally left blank]

Program:
Nuclear Power

About EPRI

EPRI creates science and technology solutions for the global energy and energy services industry. U.S. electric utilities established the Electric Power Research Institute in 1973 as a nonprofit research consortium for the benefit of utility members, their customers, and society. Now known simply as EPRI, the company provides a wide range of innovative products and services to more than 1000 energy-related organizations in 40 countries. EPRI's multidisciplinary team of scientists and engineers draws on a worldwide network of technical and business expertise to help solve today's toughest energy and environmental problems.

EPRI. Electrify the World

© 2003 Electric Power Research Institute (EPRI), Inc. All rights reserved. Electric Power Research Institute and EPRI are registered service marks of the Electric Power Research Institute, Inc. EPRI. ELECTRIFY THE WORLD is a service mark of the Electric Power Research Institute, Inc.

Printed on recycled paper in the United States of America

1003660NP

EPRI • 3412 Hillview Avenue, Palo Alto, California 94304 • PO Box 10412, Palo Alto, California 94303 • USA
800.313.3774 • 650.855.2121 • askepri@epri.com • www.epri.com